

**Aus dem Institut für Biosynthese neuraler Strukturen
des Zentrums für Molekulare Neurobiologie
des Universitätsklinikums Hamburg-Eppendorf
Direktorin: Frau Prof. Dr. Melitta Schachner**

**Quantitative morphological analysis of the
neostriatum and the cerebellum of tenascin-C
deficient mice**

Dissertation

**zur Erlangung des Grades eines Doktors der Medizin
dem Fachbereich Medizin der Universität Hamburg vorgelegt von**

Janina Alexandra Förster

aus Hamburg

Hamburg 2008

Angenommen vom Fachbereich Medizin

der Universität Hamburg am: 25.11.2008

Veröffentlicht mit Genehmigung des Fachbereichs

Medizin der Universität Hamburg

Prüfungsausschuss, der/die Vorsitzende: Prof. Dr. M. Schachner

Prüfungsausschuss: 2. Gutachter/in: PD Dr. A. Irintchev

Prüfungsausschuss: 3. Gutachter/in: Prof. Dr. M. Glatzel

CONTENTS

1 INTRODUCTION.....	6
1.1 Tenascin-C	6
1.1.1 Molecular structure and cell surface receptors.....	6
1.1.2 Expression pattern	9
1.1.3 Function	10
1.2 Tenascin-C deficient mice	11
1.2.1 Morphology.....	11
1.2.2 Physiology.....	12
1.2.3 Behaviour and neurochemistry.....	13
1.3 Tenascin-C in humans	13
2 RATIONALE AND AIM OF THE STUDY.....	15
3 MATERIALS AND METHODS	16
3.1 Animals.....	16
3.2 Preparation of tissue for sectioning.....	16
3.3 Preparation of cryostat sections	17
3.4 Antibodies.....	17
3.5 Immunofluorescence staining	18
3.6 Stereological analysis of defined cell types.....	18
3.7 Estimation of the volume of the striatum and layer thickness of the cerebellum	20
3.8 Quantitative analysis of Purkinje cell size and perisomatic and dendritic puncta of Purkinje cells (Synaptic coverage)	20
3.9 Photographic documentation	21
3.10 Statistical analysis	21
4 RESULTS.....	23
4.1 Immunohistochemical markers, quality of staining and qualitative observations for TNC+/+ and TNC-/- animals	23
4.2 Stereological analyses of the striatum	26
4.2.1 Volume of the striatum	26
4.2.2 Total cell density	26
4.2.3 Total neuronal population	27

4.2.4 Interneurons.....	28
4.2.4.1 Parvalbumin-positive interneurons	28
4.2.4.2 Cholinergic interneurons	28
4.2.5 Glial cells	29
4.2.5.1 Oligodendrocytes	29
4.2.5.2 Astrocytes.....	30
4.2.5.3 Microglia	31
4.3 Stereological analyses of the cerebellum.....	32
4.3.1 Thickness of the molecular layer and the granular layer	32
4.3.2 Total neuronal population of the granular layer.....	33
4.3.3 Interneurons.....	34
4.3.3.1 PV/NeuN-positive interneurons (stellate and basket cells).....	34
4.3.3.2 Purkinje neurons	34
4.3.4 Glial cells	35
4.3.4.1 Oligodendrocytes in the granular layer	35
4.3.4.2 Astrocytes.....	36
4.3.4.3 Microglia	38
4.4 Purkinje cell size and synaptic inputs to Purkinje cells.....	39
4.4.1 Purkinje cell size.....	39
4.4.2 Perisomatic puncta.....	40
4.4.3 Dendritic puncta	40
5 DISCUSSION	42
5.1 Gross morphological variables.....	43
5.2 Stereological analysis of defined cell populations	44
5.2.1 Genotype-related aberrations of interneuron density in the striatum	45
5.2.2 Genotype-related aberrations of interneuron density in the cerebellum.....	47
5.2.3 Genotype-related aberrations of glial cells in the striatum and the cerebellum.....	48
5.3 Synaptic coverage of Purkinje cells	50
5.4 Concluding remarks	51
6 SUMMARY	52
7 REFERENCES.....	54

8 ABBREVIATIONS	65
9 ACKNOWLEDGEMENT/DANKSAGUNG	68
10 CURRICULUM VITAE	69
11 EIDESSTATTLICHE VERSICHERUNG.....	70

1 INTRODUCTION

1.1 Tenascin-C

Tenascin-C (TNC) is an extracellular matrix (ECM) glycoprotein expressed in neural and non-neural tissues (Bourdon et al. 1983; Chiquet and Fambrough 1984; Chiquet-Ehrismann et al. 1986; Aufderheide et al. 1987; Mackie et al. 1987; Thesleff et al. 1987) and plays an important role in morphogenic tissue interactions (Grumet et al. 1985; Chiquet-Ehrismann et al. 1988). It was the first discovered and is the most intensively studied member of the tenascin family, a growing family of closely related ECM glycoproteins, which until now consists of six members: tenascin-C (Bourdon et al. 1983; Chiquet and Fambrough 1984), tenascin-R (Pesheva et al. 1989; Rathjen et al. 1991; Fuss et al. 1991, 1993), tenascin-W (Weber et al. 1998), tenascin-X (Bristow et al. 1993), tenascin-Y (Hagios et al. 1996) and tenascin-N (Neidhardt et al. 2003). Tenascin-C was identified in 1983 as a protein enriched in the stroma of gliomas, called glial/mesenchymal extracellular matrix protein (GMEM) (Bourdon et al. 1983), and as a myotendinous antigen (Chiquet and Fambrough 1984). It was also independently discovered by several other laboratories, which is why tenascin-C is also known as hexabrachion (Erickson and Inglesias 1984), cytotactin (Grumet et al. 1985), J1 220/200 (Kruse et al. 1985) and neureonectin (Rettig et al. 1989).

1.1.1 Molecular structure and cell surface receptors

Tenascin-C is a large, oligomeric molecule of 1900 kDa in humans (Taylor et al. 1989), and consists of six identical subunits (polypeptide arms) built from variable numbers of repeated domains. The six polypeptide arms are attached to a central globular core thus forming a six-armed molecule, which explains why tenascin-C is also called hexabrachion. After rotary shadowing it can be visualized in the electron microscope (Erickson and Inglesias 1984) (Fig. 1A).

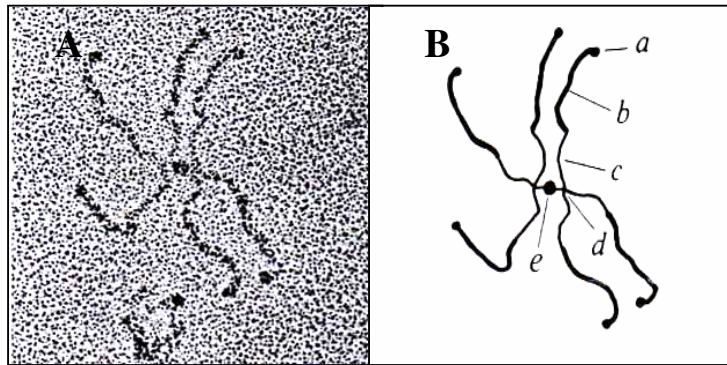


Figure 1: A: Rotary shadowed electron micrograph of human hexabrachion. B: Diagram of the common structural features: a, the terminal knob on each arm; b, the thick distal segment, ~55 nm long; c, the thin inner segment, ~30 nm long; d, two T-junctions, each with three arms; and e, the central globular particle. Magnification, $\times 250000$ (Erickson and Inglesias 1984).

The proximal parts of the arms are thin, the distal parts are thick, and their ends contain an electron dense globular particle. There seem to be two foci or attachment points on opposite sides of the globular core, with three arms extending from each focus, forming a T-junction (Erickson and Inglesias 1984, Chiquet-Ehrismann et al. 1988) (Fig. 1B).

The six polypeptide arms are linked at their amino termini via a tenascin assembly (TA) domain (Jones and Jones 2000), containing cysteine residues and three to four α -helical heptad repeats (Conway and Parry 1991). Proceeding in carboxyl termination direction follows a linear array of epidermal growth factor-like (EGFL) repeats, $13 \frac{1}{2}$ in chicken and $14 \frac{1}{2}$ in humans and mice, these being 31 amino acids in length (Nies et al. 1991; Siri et al. 1991). Adjacent to these repeats there are segments of approximately 90 amino acids similar to the type III units found in fibronectin (Jones et al. 1988; Nies et al. 1991). Eight fibronectin type III (FNIII) domains are found in all variants of TNC, but the molecule can be enlarged by additional alternatively spliced domains (Spring et al. 1989; Jones and Jones 2000). The end of the polypeptide chains is formed by a terminal knob, its structure resembling the carboxyl terminal portion of the beta and gamma chains of fibrinogen (Jones et al. 1988; Nies et al. 1991) (Fig. 2).

The other tenascins show a similar linear arrangement, but TNC is the only family member known to form hexabrachions.

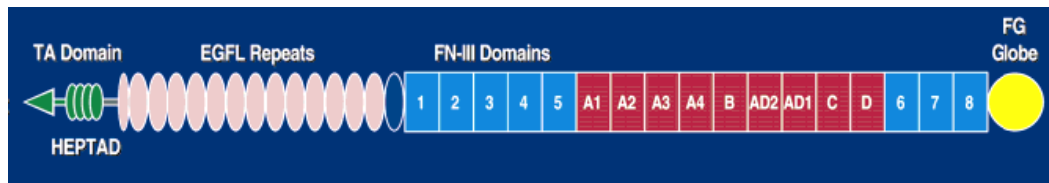


Figure 2: Schematic diagram of a TNC polypeptide arm: the tenascin assembly (TA) domain with amino terminal cysteine residues (green triangle) and heptad repeats (green hubs); an array of 13 ½ EGFL repeats (salmon-colored ovals), an additional EGFL repeat being found in mammalian species (navy-blue oval); two types of FNIII domains (1) those conserved in all variants of TNC (light blue rectangles) and (2) those that are alternatively spliced (red rectangles); and the terminal fibrinogen globe (yellow circle) (Jones and Jones 2000).

Alternative RNA splicing yields various isoforms of tenascin-C with different numbers of segments. It is one way to select for binding of particular cell types via preferential interactions with cellular receptors or ECM components, thereby generating considerable diversity in the function of TN-polypeptides (Jones and Jones 2000). Splicing mainly occurs between the fifth and the sixth FNIII domain of the basic structure (Spring et al. 1989; Nies et al. 1991). FNIII domains around the proximal splice site influence neuronal migration and repeats around the distal splice site promote neurite outgrowth (Faissner et al. 1994; Faissner and Steindler 1995). The EGFL repeats play a role in neuronal migration and pathfinding during development of the central nervous system (CNS) (Jones and Jones 2000).

Cell surface receptors for tenascins include members of the integrin family (Prieto et al. 1992), cell adhesion molecules (CAMs) of the immunoglobulin superfamily, a transmembrane receptor called phosphacan/receptor protein tyrosine phosphatase beta/zeta (RPTP z/b) (Barnea et al. 1994; Milev et al. 1997), and annexin II (Chung und Erickson 1994; Chung et al. 1996). TNC is also known to interact with other extracellular proteins, including fibronectin (Chiquet-Ehrismann 1991; Chung et al. 1995) and extracellular chondroitin sulphate proteoglycans (Chiquet and Fambrough 1984; Vaughan et al. 1987).

1.1.2 Expression pattern

TNC is highly expressed during organogenesis of almost every organ. Its expression is down-regulated in most adult tissues, but TNC reappears under pathological conditions such as infection, inflammation, wound healing and tumourigenesis (Erickson and Bourdon 1989; Chiquet-Ehrismann et al. 1995; Chiquet-Ehrismann and Chiquet 2003).

In the central nervous system, tenascin-C is widely expressed at early stages of development (Crossin et al. 1989; Bartsch et al. 1992; Götz et al. 1997; Joester and Faissner 1999). Its expression can first be observed at the stages of gastrulation and somite formation (Crossin et al. 1986). Subsequently the glycoprotein is detected in distinct areas of the developing CNS where its expression can be correlated with key events of neurohistogenesis such as cell proliferation in the ventricular and subventricular zone, neuronal migration, segregation of neuronal assemblies and extension of neuronal processes (Steindler 1993; Gates et al. 1995; Bartsch 1996; Götz et al. 1997). A typical feature of tenascin-C expression is its boundary-like expression, as seen in the striatal mosaic and barrel cortex (Steindler et al. 1989; O'Brien et al. 1992). At times of further differentiation and maturation of the CNS, TNC is down-regulated (Crossin et al. 1989; Bartsch et al. 1992; Joester and Faissner 1999) so that the protein is only present in a few brain regions in the adult animal, e.g. the molecular layer of the cerebellum (Bartsch et al. 1992), the subventricular zone (Gates et al. 1995), the olfactory bulb (Miragall et al. 1990), the retina (Bartsch et al. 1994) and the hippocampus (Ferhat et al. 1996), areas distinctive of neuronal plasticity or active neurogenesis. Expression of TNC has been reported as being up-regulated again after lesions of the CNS (Laywell et al. 1992; Brodkey et al. 1995; Bartsch 1996).

Tenascin-C is mainly produced by immature astrocytes, in particular radial glial cells and Bergmann glial cells, during neuronal differentiation and migration in the cortex and cerebellum (Crossin et al. 1986; Prieto et al. 1990; Tucker et al. 1994; Yuasa 1996). The molecule is also produced by neuronal subpopulations localized in the hippocampus, the spinal cord and the retina (Bartsch 1996; Götz et al. 1996).

1.1.3 Function

TNC has many functions, but it is predominantly involved in tissue development and repair. In numerous studies it has been documented to be adhesive (Grumet et al. 1985; Bourdon and Ruoslahti 1989; Aukhil et al. 1990; Prieto et al. 1992) or anti-adhesive (Faissner und Kruse 1990; Prieto et al. 1992) for glial cells and neurons. Such apparently opposing activities may be due to the multidomain structure of tenascin-C, in which the adhesive and anti-adhesive activities are mapped to different FNIII domains and EGFL repeats (Götz et al. 1996).

Its adhesive and anti-adhesive properties enable TNC to modulate cell proliferation. It might stimulate cell proliferation *in vitro*, e.g. of smooth muscle cells (Cleek et al. 1997; Cowan et al. 2000), and *in vivo* (see 1.2.1), but the glycoprotein has also been found to inhibit cell proliferation (Crossin 1991). It is documented as acting as a survival factor by suppressing apoptosis (Cowan et al. 2000), while on the other hand, studies on tenascin-C deficient mice report that TNC deficiency leads to reduced levels of programmed cell death, which might indicate that it is also involved in the induction of apoptosis (Garcion et al. 2001).

The duality of adhesive and repulsive properties should also predispose TNC to participate in the control of cell migration, which is characterised by the dichotomy of bond formation and subsequent release (Faissner 1997). In agreement with this assumption, the protein has been found to modulate the motility of many cell types. It stimulates migration, for example, of cerebellar granule cells from the external to the internal granular cell layer, a key event of postnatal cerebellar development (Chuong et al. 1987; Bartsch et al. 1992; Husmann et al. 1992). And it has been shown that after *in vivo* knockdown of tenascin-C with morpholino antisense oligonucleotides, neural crest cells migrate abnormally (Tucker 2001). In contrast to granule and crest cells, TNC reduces the motility of satellite cells derived from embryonic chicken dorsal root ganglia (Wehrle-Haller and Chiquet 1993).

Additionally, tenascin-C is involved in axonal growth and guidance. Promotion of neurite outgrowth (Crossin et al. 1990; Husmann et al. 1992; Lochter and Schachner 1993; Taylor et al. 1993; Faissner and Steindler 1995), but also deflection of growth cones of embryonic mesencephalic neurones, embryonic hippocampal neurones and postnatal cerebellar neurones (Crossin et al. 1990; Faissner and Kruse 1990; Taylor et

al. 1993; Faissner and Steindler 1995), has been documented. The influence of the glycoprotein on growth cone motility depends on the neuronal cell type and the expression pattern, i.e. as a uniform substrate or as a substrate boundary. For example, when tenascin-C is offered as a sharp substrate boundary with tenascin-R (TNR), growth cone neurons of both retinal and dorsal root ganglion cells avoid growing on this substrate, but are not induced to collapse. When TNC and TNR are offered in a mixture with laminin as a uniform substrate, however, dorsal root ganglion growth cones display a collapsed morphology and are able to advance at a faster rate than on laminin alone. The outgrowth of retinal ganglion neuron growth cones, by contrast, is completely inhibited under these conditions (Taylor et al. 1993).

TNC plays a role in various regenerative processes, such as peripheral nerve regeneration and wound healing in the brain (Irintchev et al. 1993; Martini 1994; Langenfeld-Oster et al. 1994; Brodkey et al. 1995). It also regulates the phenotype of cultured astrocytes *in vitro*, thus possibly regulating astrocytic scar formation after spinal cord injury (Holley et al. 2005).

1.2 Tenascin-C deficient mice

To directly assess the function of tenascin-C *in vivo*, mutant mice deficient in TNC (TNC^{-/-} mice) have been generated in several laboratories (Saga et al. 1992; Forsberg et al. 1996; Evers et al. 2002). These mice appear normal and are viable and fertile.

1.2.1 Morphology

The gross-anatomical appearance of the tenascin-C deficient mouse is normal. Neither differences in cell architecture nor other histological abnormalities have been found, on analysing a variety of tissues with hematoxylin-eosin staining (Saga et al. 1992). Later studies found morphological aberrations in TNC deficient mice. Abnormal structure of the neuromuscular junction and peripheral nerves has been documented by Cifuentes-Diaz et al. (1998; but see Moscoso et al. 1998 for lack of pathology in the peripheral nervous system). Other subtle differences have been

detected in the CNS during investigations of the motor and sensory cortex. It is said that TNC deficient mice show the typical six-layer organization of the cortex, but they also show variations in the numbers of several cell types, namely, a significantly lower density of parvalbumin-positive interneurons and higher densities of neurons and astrocytes (Irintchev et al. 2005). A higher density of astrocytes has also been found in the hippocampus of the mutant mouse (F. Kuang, A. Irintchev, personal communication).

Defects in different regenerative processes have been detected in the TNC^{-/-} mice, e.g. impaired recovery of functions following facial nerve transection and surgical repair (Guntinas-Lichius et al. 2005), and failure to regenerate from Habu-snake venom-induced glomerulonephritis (Nakao et al. 1998). TNC ablation in mice leads to an increased migration rate of oligodendrocyte precursor cells along the optic nerve (Garcion et al. 2001). This effect is indirectly mediated by the effects of TNC deficiency on the ECM, because the addition of purified tenascin-C does not reduce the migration rate to wild-type levels. In addition, reduced rates of oligodendrocyte precursor proliferation have been detected in other regions of the CNS, such as the cortex, the corpus callosum and the striatum. This effect has been found to be accompanied by reduced levels of cell death in prospective white matter during later developmental stages, providing a potential compensatory mechanism in terms of cell number.

1.2.2 Physiology

Abnormalities in synaptic transmission and plasticity in the hippocampus have been detected by electrophysiological measurements in TNC deficient mutants. Theta-burst stimulation of Schaffer collaterals elicits reduced long-term potentiation (LTP) in the CA1 region of the mutant mouse as compared to the wild-type littermate (Evers et al. 2002). Whereas high-frequency stimulation evokes normal LTP in TNC^{-/-} mice, low-frequency stimulation fails to induce long-term depression in the CA1 region. It has been suggested that these deficits result from a reduction in L-type voltage-dependent Ca²⁺ channel-mediated signalling (Evers et al. 2002). Additionally, abnormalities in short-term plasticity in synapses on Purkinje cells have been found in

TNC deficient mice (Andjus et al. 2005). Compared to wild-type animals, climbing fibre paired-pulse depression is less pronounced in tenascin-C deficient mice, while parallel fibre paired-pulse facilitation is augmented in some mutant mice, but depressed in others.

It has also been reported that mice lacking TNC show early impairments in olfactory detection (de Chevigny et al. 2006).

1.2.3 Behaviour and neurochemistry

TNC knockout mice generated by Saga et al. (1992) display abnormal behaviour, such as hyperlocomotion and poor swimming ability (Fukamauchi et al. 1996). This may derive from low levels of dopamine transmission in the striatum or the hippocampus (Fukamauchi et al. 1996; Fukamauchi and Kusakabe 1997) which are at least partly due to the reduced tyrosine hydroxylase (TH) activity in TNC deficient mice (Fukamauchi et al. 1997). Levels of preprotachykinin A and cholecystokinin mRNAs, assayed in the terminal fields of the dopamine neurons, have been found to be increased in the mutant mice. This probably reflects a functional compensation against the low level of dopamine turnover rate in the TNC knockout mouse brain (Fukamauchi and Kusakabe 1997). These mice also have poor appetite and abnormal circadian rhythm. This is in good agreement with the observed reduction of the neuropeptide Y levels, which affects emotions, circadian rhythm and food intake (Fukamauchi et al. 1998). Another TNC knockout mouse, which is a true TNC-null mouse (Evers et al. 2002), as opposed to the mutant generated by Saga and colleagues, has shown enhanced novelty-induced activity, reduced anxiety, weaker grip strength (Morellini and Schachner 2006) and deficits in coordination during beam walking (Kiernan et al. 1999).

1.3 Tenascin-C in humans

In the human brain, TNC is expressed predominantly in the white matter, especially in the ECM, and only rarely in blood vessels (Leins et al. 2003). It is found in the white matter of the frontal, temporal, parietal, and occipital lobes and in the

hippocampus. TNC is also expressed to various extents in the cellular and stromal components of brain tumours and tumour-associated vessels (Leins et al. 2003). The human TNC gene is localized on chromosome 9 in band q32-q34 (Rocchi et al. 1991).

2 RATIONALE AND AIM OF THE STUDY

The extracellular matrix protein tenascin-C has been implicated in neural development and plasticity, but many of its functions *in vivo* remain obscure. Aberrations in cellular populations in the motor and sensory cortex of adult TNC-/- mice have already been detected by Irintchev et al. (2005). In this study, we have focused on two other brain regions in the adult TNC deficient mouse: the cerebellum and the neostriatum (referred to, for simplicity, as striatum throughout the text). Both are specifically important for control of movement and posture, and execution of motor programmes (Trepel 1995). Since behavioural abnormalities have been found in TNC deficient mice, investigations of these brain regions seemed especially warranted. Concerning the structure of the striatum and the cerebellum, particular questions were whether:

1. TNC deficiency causes changes in the gross structure (volume) of the striatum and cerebellum;
2. TNC deficiency causes alterations in the size of major neuronal or glial populations.

To answer these questions precisely, an established quantitative (stereological) approach was applied (Irintchev et al. 2005). It is based on immunohistochemical visualization of defined cell types such as subpopulations of interneurons, astrocytes, oligodendrocytes and microglia, and stereological estimation of cell densities and volumes of structures.

3 MATERIALS AND METHODS

3.1 Animals

The TNC deficient (TNC^{-/-}) and wild-type (TNC^{+/+}) mice used in this study were offspring of heterozygous (TNC^{+/-}) parents and had a C57BL/6J-129SvJ genetic background (Evers et al. 2002). The animals were bred at the specific, pathogen-free animal facility of the Universitätsklinikum Hamburg. Six wild-type and 6 knockout mice at the age of 5 months (adult mice) were investigated. All animals appeared healthy before being sacrificed for morphological analyses. Animal treatments were performed in accordance with the German law on protection of experimental animals. All technical procedures described below were performed as described previously (Irintchev et al. 2005).

3.2 Preparation of tissue for sectioning

Mice were anaesthetized with a 16% w/v (weight/volume) solution of sodium pentobarbital (Narcoren®, Merial, Hallbermoos, Germany, 5 µl/g body weight, i.p.). Once surgical tolerance had been achieved, the animals were transcardially perfused with physiological saline for 60 s followed by fixative (4% w/v formaldehyde and 0.1% w/v CaCl₂ in 0.1 M cacodylate buffer, pH 7.3, 15 min at room temperature, RT). Cacodylate buffer supplemented with calcium was selected to ensure optimal tissue fixation including preservation of highly soluble antigens, such as S-100 (Rickmann and Wolff 1995). Following perfusion, the brains were left in situ for 2 h at RT to reduce fixation artefacts (Garman 1990) and then dissected out without the olfactory bulbs and post-fixed overnight (18-22 h) at 4°C in the formaldehyde solution used for perfusion, supplemented with 15% w/v sucrose. Tissue was then immersed into 0.1 M cacodylate buffer containing 15% sucrose, pH 7.3, for 18-24 hours at 4°C.

The fixed and cryoprotected (sucrose-infiltrated) brains were carefully examined under a stereomicroscope and hairs, rests of dura mater and other tissue debris were removed using fine forceps. Afterwards, they were placed into a mouse brain matrix (World Precision Instruments, Berlin, Germany) and the caudal end was cut at a

defined level (1 mm from the most caudal slot of the matrix). Finally, the tissue was frozen for 2 min in 2-methyl-butane (isopentane) precooled to -30°C in the cryostat and stored in liquid nitrogen until sectioned.

3.3 Preparation of cryostat sections

For sectioning, the rostral pole of each brain was attached to a cryostat specimen holder using a drop of distilled water placed on a pre-frozen layer of TissueTek® (Sakura Finetek Europe, Zoeterwoude, The Netherlands). The ventral surface of the brain was oriented so as to face the cryostat knife edge and serial coronal sections of $25\ \mu\text{m}$ thickness were cut in a caudal-to-rostral direction on a cryostat (Leica CM3050, Leica Instruments, Nußloch, Germany). Sections taken from 1 mm thick tissue ($40 \times 25\ \mu\text{m}$) were picked up on a series of ten SuperFrost®Plus glass slides (Roth, Karlsruhe, Germany) so that four sections $250\ \mu\text{m}$ apart were present on each slide. Finally, the sections were air-dried for at least 1 h at RT and stored in boxes at -20°C until stainings were performed.

3.4 Antibodies

The following commercially available antibodies were used in optimal dilutions: anti-parvalbumin (PV, mouse monoclonal, clone PARV-19, Sigma, Taufkirchen, Germany, dilution 1:1000), anti-NeuN (mouse monoclonal, clone A60, Chemicon, Hofheim, Germany, 1:1000), anti-ChAT (goat polyclonal, Chemicon, 1:100), anti-calbindin (CB, rabbit polyclonal, affinity purified, Sigma, 1:1000), anti-cyclic nucleotide phosphodiesterase (CNPase, mouse monoclonal, clone 11-5B, Sigma, 1:1000), anti-S-100 (rabbit polyclonal, purified IgG fraction, DakoCytomation, Hamburg, Germany, 1:500 for striatum and 1:2000 for cerebellum), anti-Iba1 (rabbit polyclonal, affinity purified, Wako Chemicals, Neuss, Germany, 1:1500) and anti-vesicular GABA transporter (VGAT, rabbit polyclonal, affinity purified, Synaptic Systems, Göttingen, Germany, 1:1000).

3.5 Immunofluorescence staining

Sections stored at -20°C were air-dried for 30 min at 37°C . Afterwards they were incubated for 30 minutes in a 0.01 M sodium citrate solution (pH 9.0, adjusted with 0.01 M NaOH) which had been preheated to 80°C in a water bath for antigen retrieval (Jiao et al. 1999). When the slides had cooled down to room temperature, non-specific binding sites were blocked using phosphate-buffered saline (PBS, pH 7.3) containing 0.2% v/v Triton X-100 (Fluka, Buchs, Germany), 0.02% w/v sodium azide (Merck, Darmstadt, Germany) and 5% v/v normal goat or donkey serum (Jackson Immuno Research Laboratories, Dianova, Hamburg, Germany) for 1 h at RT. The selection of normal serum for blocking was determined on the basis of the species in which the secondary antibody was produced (see below). Following aspiration of the blocking solution, incubation with the primary antibody, diluted in PBS containing 0.5% w/v lambda-carrageenan (Sigma) and 0.02% w/v sodium azide, was carried out for 3 days at 4°C . After wash in PBS (3 x 15 min at RT), the appropriate (anti-rabbit, anti-mouse or anti-goat) secondary antibody diluted 1:200 in PBS-carrageenan solution was applied for 2 h at RT. Goat anti-rabbit, goat anti-mouse or donkey anti-goat IgG conjugated with Cy3 (Jackson Immuno Research Laboratories, Dianova, Hamburg, Germany) was used. After a subsequent wash in PBS, cell nuclei were stained for 10 min at RT with bis-benzimide solution (Hoechst 33258 dye, 5 $\mu\text{g}/\text{ml}$ in PBS, Sigma). Finally, the sections were washed again, mounted in anti-fading medium (Fluoromount G, Southern Biotechnology Associates, Biozol, Eching, Germany) and stored in the dark at 4°C . Specificity of staining was tested by omitting the first antibody or replacing it by variable concentrations of normal serum or IgG. All these controls were negative.

3.6 Stereological analysis of defined cell types

The numerical densities of a variety of cell types were quantified using the optical dissector method (Irintchev et al. 2005). Objects are directly counted in relatively thick sections (25 μm) under the microscope using a three-dimensional counting frame (dissector) to “probe” the tissue at random. The base of the frame

(dimensions in the x/y plane) is defined by the size of the squares formed by a grid projected into the visual field of the microscope. The height of the dissector is a portion of the section thickness defined by two focal planes in the z axis at a distance of $x \mu\text{m}$. Objects (e.g. cells) within each dissector are counted according to stereological rules; those entirely within the dissector, as well as those touching or being dissected by the “acceptance” but not the “forbidden” planes of the frame, are counted (Howard and Reed 1998).

Counting was performed on an Axioskop microscope (Zeiss, Oberkochen, Germany) equipped with a motorized stage and NeuroLucida software-controlled computer system (MicroBrightField, Colchester, USA). Sections containing the striatum or the cerebellum were identified at low magnification (Plan-Neofluar® 10x/0.3 objective) by viewing the nuclear staining, a 365/420 nm excitation/emission filter set (01, Zeiss, blue fluorescence) being used. The area viewed was randomised by setting an arbitrary reference point, resulting in a grid-overlay of the visible field with lines spaced at 30 μm (for investigations of all cells and all neurons in the striatum and granule cells of the cerebellum) or 60 μm (for all other cell populations studied). The contours of the areas of interest were outlined with the cursor and squares with defined separation distances (180 μm : PV, ChAT, Iba1, CNPase and S-100 (striatum), S-100 (cerebellum); 120 μm : NeuN and Iba1 (cerebellum, molecular layer); 90 μm : all cells and NeuN (striatum); 60 μm : CB (cerebellum), CNPase and Iba1 (cerebellum, granular layer); 30 μm : NeuN (cerebellum, granular layer)) within this area were marked for counting, starting from the uppermost left side of the delineated field. A dissector depth of 10 μm appeared appropriate since antibody penetration was sufficient to enable clear recognition of stained objects to a depth of at least 15 μm . The guard depth was determined as 2 μm . The sections were then viewed at a magnification of 40 (Plan-Neofluar® 40x/0.75 objective) and with a 546/590 nm excitation/emission filter set (15, Zeiss, red fluorescence). Immunolabelled cell profiles that were entirely within the counting frame at any focus level, as well as those touching or being dissected by the acceptance planes, were marked and their nuclei were identified in the blue filter set. All nuclei that were in focus beyond the guard space, i.e. lying within 2 and 12 μm below the surface of the section, were counted, except for those touching the level of 2 μm (“look-up” level). Four sections spaced 250 μm apart were examined per staining

and animal in the striatum. For both genotypes, the number of samples from the left and the right hemisphere was roughly equal. In the cerebellum, two cortical fields extending for approximately 500 μm on both sides of the sagittal line were analyzed, again in four sections per staining and animal. All counts were performed on coded preparations by one observer. Values for all morphological parameters are expressed as means \pm SD.

3.7 Estimation of the volume of the striatum and layer thickness of the cerebellum

The volume of a defined segment of the striatum was estimated according to the Cavalieri principle, the most commonly used stereological method for the estimation of a reference volume (Howard and Reed 1998). According to this principle, the volume (V) of an object of interest can be estimated from its profile areas (A) on sections cut at a constant distance (T) whereby:

$$\text{est}_1 V = T(A_1 + A_2 + A_3 + \dots + A_m).$$

To determine the area of a defined segment of the striatum, four coronal sections 250 μm apart were chosen for area measurements, the most rostral of these sections being similar to Figure 33 in the brain atlas of Franklin and Paxinos (1997).

To estimate the average thickness of the molecular and the granular cell layer of the cerebellum, the area of each delineated field used for estimation of cell densities in the cerebellum was divided by the length of its boundary facing the meningeal surface (Irintchev et al. 2005).

3.8 Quantitative analysis of Purkinje cell size and perisomatic and dendritic puncta of Purkinje cells (Synaptic coverage)

Estimation of the area of Purkinje cell bodies and perisomatic puncta was performed as described previously (Irintchev et al. 2005). Stacks of images of 1 μm thickness were obtained from sections stained for VGAT on a Leica SP 2 confocal microscope (Leica, Mannheim, Germany) using a Helium Neon Laser and a 543 nm excitation filter set. A 63x oil immersion objective and 1024 x 1024 pixel digital

resolution were chosen. Each image contained a part of the Purkinje cell layer with approximately 4-8 Purkinje cells and the inner two-thirds of the molecular layer. One image per cell, at the level of the largest cell body cross-sectional area, was used to measure soma perimeter and area, and to count individually discernible perisomatic puncta. The number of VGAT⁺ puncta was normalized to the perimeter of the cell profile. These measurements were performed using the UTHSCSA ImageTool 3.0 software (University of Texas, San Antonio, Texas, USA).

The profile densities (number per unit area) of VGAT⁺ terminals in the inner two-thirds of the molecular layer (dendritic puncta) were estimated using the image stacks required for estimation of Purkinje cell size and perisomatic puncta. Single optical slices of 1 μm thickness were used to count immunolabeled dendritic puncta in 100 x 100 μm counting frames. Two randomly sampled fields in the molecular layer, one adjacent to the somata of the Purkinje cells and one approximately in the middle of the molecular layer, were analyzed in four sections per animal. These measurements were taken using Adobe Photoshop 7.0 software (Adobe System Inc., San Jose, California, USA).

3.9 Photographic documentation

The stereological analysis of cell densities was photographically documented using an Axiophot 2 microscope equipped with a digital camera AxioCam HRC and AxioVision software (Zeiss) at highest resolution (2300 x 2030 pixels, RGB). For the photographic documentation of the analysis of Purkinje cells size and Purkinje cell perisomatic and dendritic puncta, images of the stacks on which counting was performed were used. They were obtained using a Leica SP 2 confocal microscope (see above). All images were additionally processed using Adobe Photoshop 7.0 software (Adobe System Inc., San Jose, California, USA).

3.10 Statistical analysis

Group mean values were compared using SigmaPlot 8.0 software (SPSS, Chicago, Illinois, USA). A two-sided *t*-test for independent groups was chosen in

accordance with the results of tests for equal variance and normal distribution. Given two or more measurements per parameter and animal, the mean was used as a representative value. The degree of freedom for all comparisons was thus determined by the number of animals. The accepted level of significance was 5%.

4 RESULTS

4.1 Immunohistochemical markers, quality of staining and qualitative observations for TNC+/+ and TNC-/- animals

Tissue preparation and sectioning was performed in a highly reproducible manner for all animals. For a given staining, all sections were stained in the same primary and secondary antibody solutions which were kept in staining jars and stabilized by the addition of carrageenan in order to allow repeated long-term usage for a particular antigen (Irintchev et al. 2005). No qualitative differences between TNC+/+ and TNC-/- mice were noticed in the staining patterns for the detected antigens.

The antibodies used in this study recognize specific cell-marker antigens expressed in defined cell populations (Irintchev et al. 2005):

-NeuN (neuron-specific nuclear antigen) is a phosphoprotein observed in most postmitotic neuronal cell types throughout the nervous system, except for Purkinje, mitral and photoreceptor cells (Wolf et al. 1996)

-PV (parvalbumin) is a low molecular weight calcium-binding protein expressed in a major subpopulation of GABAergic neurons

-ChAT (choline acetyltransferase) is the acetylcholine-synthesizing enzyme which identifies cholinergic neurons

-Iba1 (ionized calcium-binding adaptor molecule 1) is a macrophage/microglia-specific calcium-binding protein involved in the activation of quiescent microglial cells (Imai and Kohsaka 2002)

-S-100 is a low molecular weight calcium-binding protein localized in astrocytes

-CNPase (2', 3'-cyclic nucleotide 3'-phosphodiesterase) is one of the earliest myelin-related proteins expressed in differentiating and mature oligodendrocytes

-CB (calbindin) is an intracellular calcium-binding protein that occurs only in a subset of neurons and is often used as a marker for cerebellar Purkinje cells

For quantification of perisomatic and dendritic puncta of Purkinje cells, another specific marker was used:

-**VGAT** (vesicular GABA transporter) is highly concentrated in the nerve endings of most GABAergic neurons in the brain and spinal cord, but also in glycinergic nerve endings (Chaudhry et al. 1998)

Examples of different stainings are shown in Fig. 3.

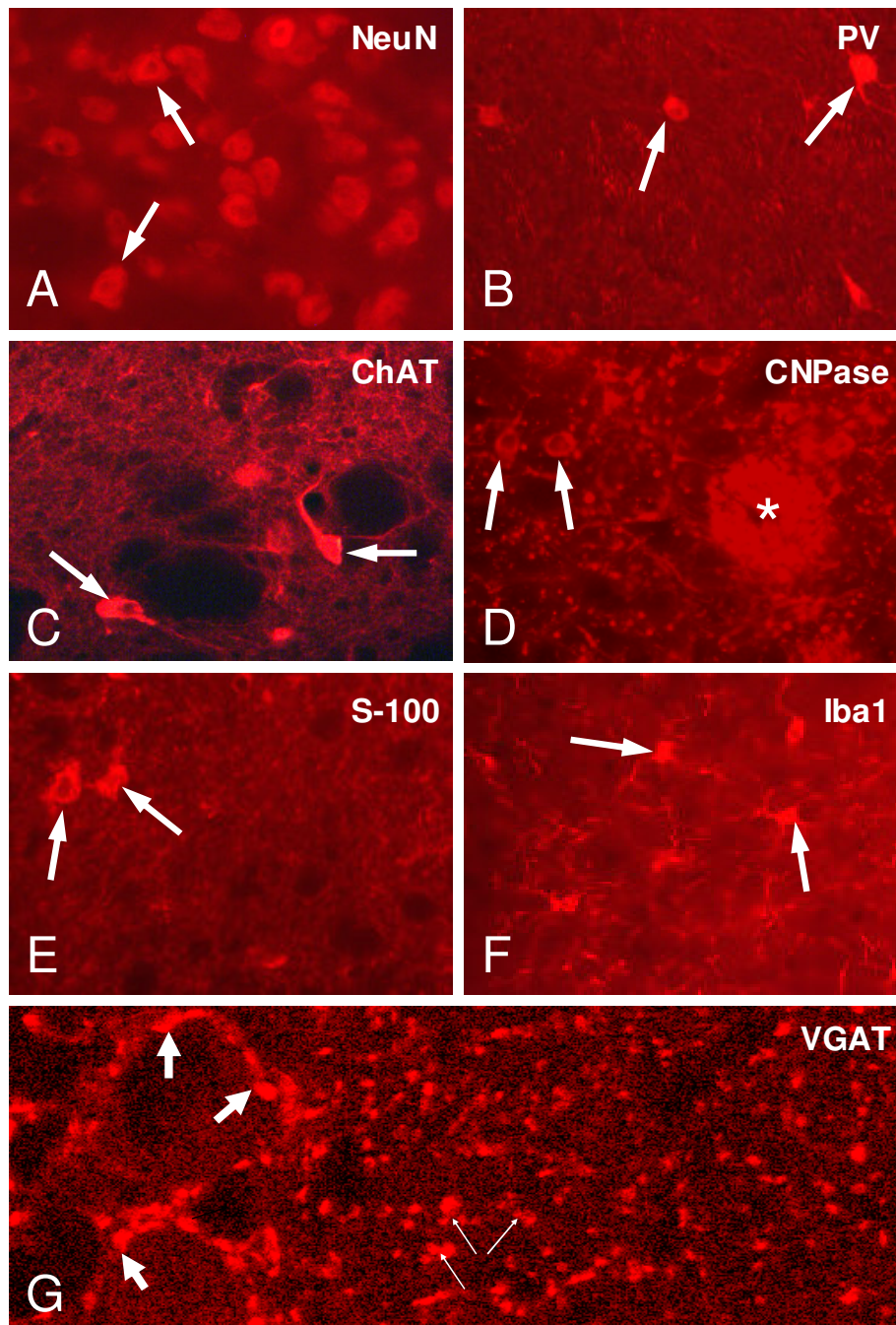


Figure 3: Examples of the immunohistochemical stainings used for quantitative analyses. Coronal brain sections from the striatum (A-F) and the cerebellum (G) of 5-month-old TNC^{-/-} (A, D, E, G) and TNC^{+/+} (B, C, F) mice. Arrows in A-F point to individual cell profiles. Arrows in G mark perisomatic puncta (thick arrows) and dendritic puncta (thin arrows). The asterisk in D indicates staining of myelinated axonal bundles for CNPase.

4.2 Stereological analyses of the striatum

4.2.1 Volume of the striatum

The volume of a defined segment of the striatum (caudate nucleus and putamen) was determined using the Cavalieri method (see above). The volume of the striatum of TNC^{-/-} mice did not differ statistically to that of TNC^{+/+} mice (Fig. 4). Differences in the densities of the following cell populations therefore reflect differences in the absolute numbers of cells.

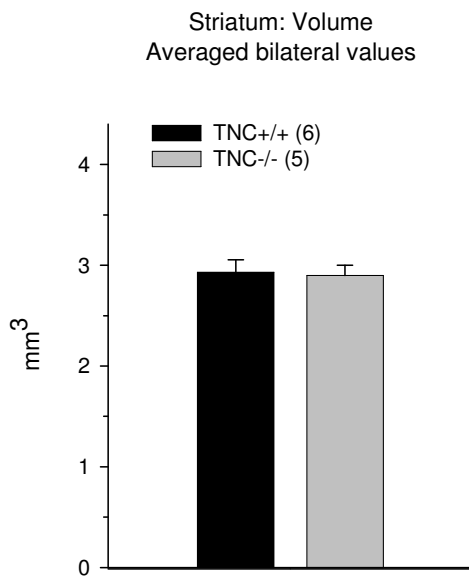


Figure 4: Volume of a defined segment of the striatum of TNC^{+/+} (black bars) and TNC^{-/-} (grey bars) animals. Shown are averaged bilateral values + SD. The number of animals studied per group is indicated in the legend. No significant difference was detected (*t*-test).

4.2.2 Total cell density

Nuclear staining was used to estimate the numerical density (i.e., number per unit volume) of all cells as a reference value indicative of global alterations in the striatum. The results showed no significant difference between TNC deficient mice and wild-type mice (Fig. 5).

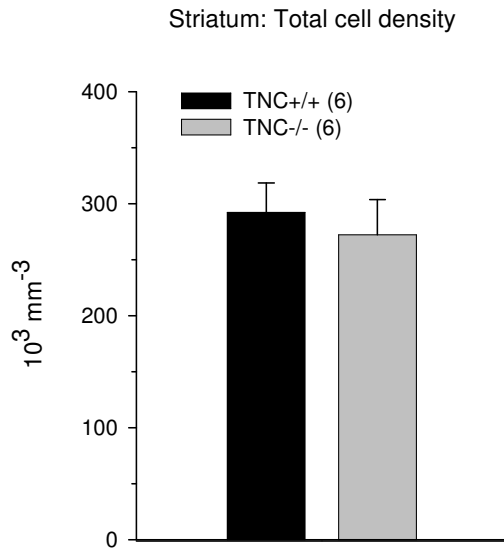


Figure 5: Total cell density in the striatum of TNC+/+ (black bars) and TNC-/- (grey bars) animals. Shown are mean values + SD. The number of animals studied per group is indicated in the legend. No significant difference was found (*t*-test).

4.2.3 Total neuronal population

The density of all neurons in the striatum, the vast majority of which are spiny projection neurons, was similar for TNC-/- and TNC+/+ mice (Fig. 6).

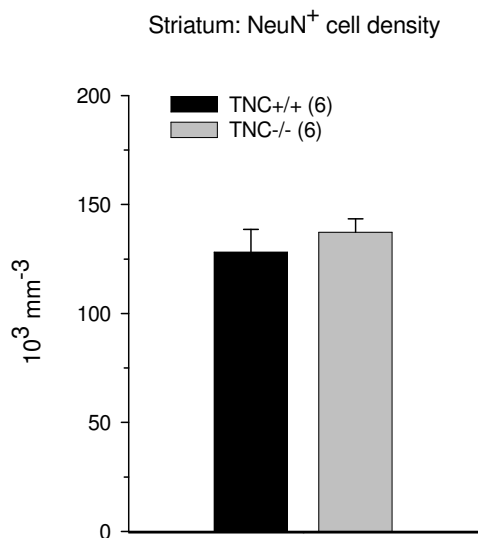


Figure 6: Neuronal density in the striatum of TNC+/+ (black bars) and TNC-/- (grey bars) animals. Shown are mean values + SD. The number of animals studied per group is indicated in the legend. No significant difference was found (*t*-test).

4.2.4 Interneurons

4.2.4.1 Parvalbumin-positive interneurons

The density of PV-positive interneurons was significantly lower (-21%) in the mutant mice (Fig. 7). This is in agreement with findings in the motor and sensory cortex, where the density of PV⁺ cells was 25% lower in TNC^{-/-} mice (Irintchev et al. 2005).

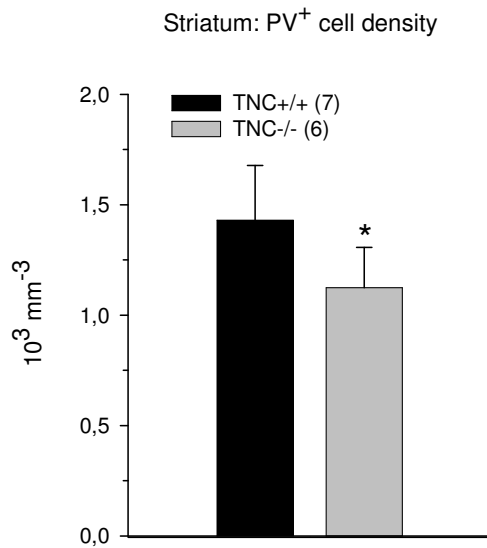


Figure 7: Density of parvalbumin-positive interneurons in the striatum of TNC^{+/+} (black bars) and TNC^{-/-} (grey bars) animals. Shown are mean values + SD. The number of animals studied per group is indicated in the legend. The asterisk indicates a significant difference between the two groups (*t*-test).

4.2.4.2 Cholinergic interneurons

The mean density of ChAT-positive cells in the striatum was similar for both groups (Fig. 8).

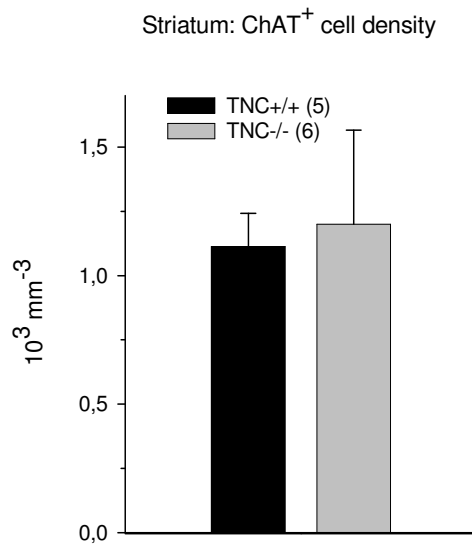


Figure 8: Density of cholinergic interneurons in the striatum of TNC^{+/+} (black bars) and TNC^{-/-} (grey bars) animals. Shown are mean values + SD. The number of animals studied per group is indicated in the legend. No significant difference was detected (*t*-test).

4.2.5 Glial cells

4.2.5.1 Oligodendrocytes

No significant genotype-related difference in the density of oligodendrocytes was detected (Fig. 9).

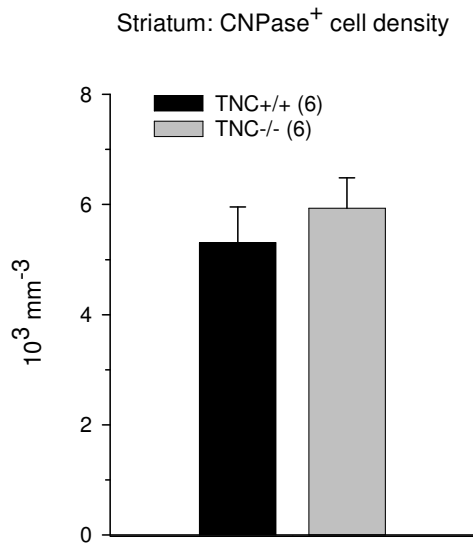


Figure 9: Density of oligodendrocytes in the striatum of TNC^{+/+} (black bars) and TNC^{-/-} (grey bars) animals. Shown are mean values + SD. The number of animals studied per group is indicated in the legend. No significant difference was found (*t*-test).

4.2.5.2 Astrocytes

The density of S-100⁺ cells was significantly higher (+20%) in the TNC^{-/-} mice (Fig. 10). This is in good agreement with results of investigations of the neocortex (Irintchev et al. 2005) and the hippocampus (F. Kuang, A. Irintchev, personal communication), where the density of astrocytes has also been found to be higher in TNC deficient animals.

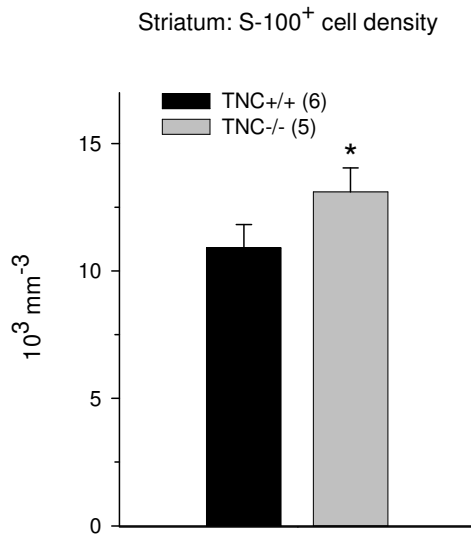


Figure 10: Density of astrocytes in the striatum of TNC^{+/+} (black bars) and TNC^{-/-} (grey bars) animals. Shown are mean values + SD. The number of animals studied per group is indicated in the legend. The asterisk indicates a significant difference between the two groups (*t*-test).

4.2.5.3 Microglia

No difference in microglial cell density between TNC^{-/-} mice and wild-type littermates was found (Fig. 11).

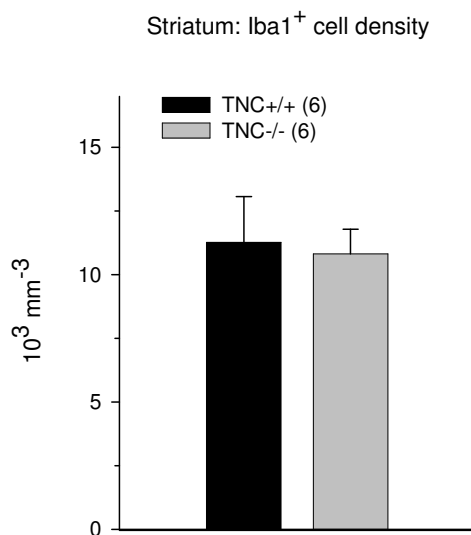


Figure 11: Density of microglial cells in the striatum of TNC^{+/+} (black bars) and TNC^{-/-} (grey bars) animals. Shown are mean values + SD. The number of animals studied per group is indicated in the legend. No significant difference was found (*t*-test).

4.3 Stereological analyses of the cerebellum

4.3.1 Thickness of the molecular layer and the granular layer

The normalized thickness was calculated as a ratio of the layer segment area to the length of the surface boundary of the segment. Layer thickness was similar in the two genotype groups in both the molecular layer (Fig. 12) and the granular layer (Fig. 13), an observation which is in agreement with the determination of a normal thickness for the granular layer by Saga et al. (1992). This finding is important with regard to the interpretation of differences in cell densities in terms that, as for the striatum, cell densities reflect absolute cell numbers.

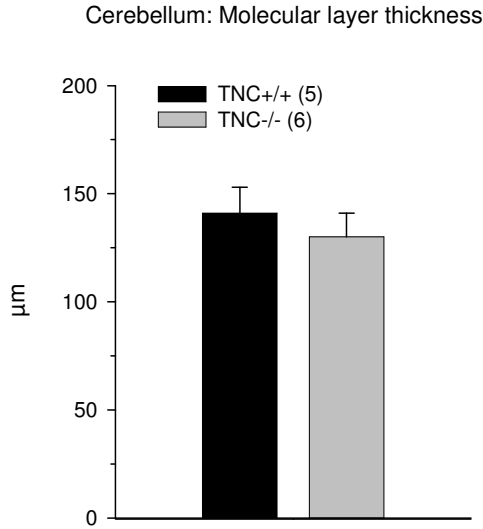


Figure 12: Thickness of the molecular layer in the cerebellum of TNC+/+ (black bars) and TNC-/- (grey bars) animals. Shown are mean values + SD. The number of animals studied per group is indicated in the legend. No significant difference was found (*t*-test).

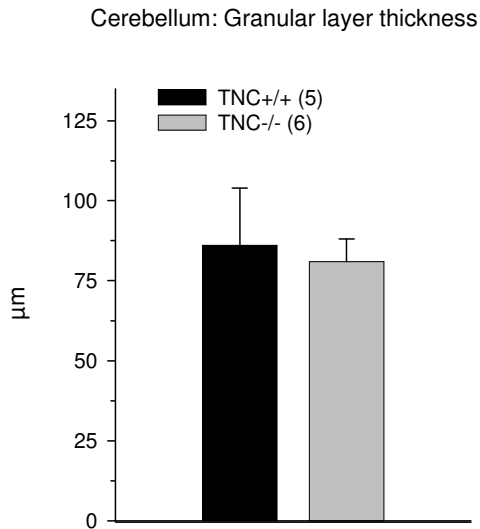


Figure 13: Thickness of the granular layer in the cerebellum of TNC+/+ (black bars) and TNC-/- (grey bars) animals. Shown are mean values + SD. The number of animals studied per group is indicated in the legend. No significant difference was detected (*t*-test).

4.3.2 Total neuronal population of the granular layer

The neuronal density in the granular layer (NeuN staining), which consists mainly of densely packed granule cells, was found to be similar for TNC-/- and TNC+/+ mice (Fig. 14).

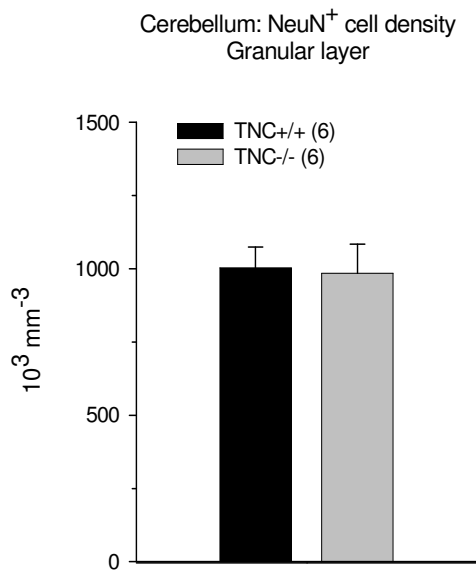


Figure 14: Total neuronal cell density in the granular layer of the cerebellum of TNC+/+ (black bars) and TNC-/- (grey bars) animals. Shown are mean values + SD. The number of animals studied per group is indicated in the legend. No significant difference was detected (*t*-test).

4.3.3 Interneurons

4.3.3.1 PV/NeuN-positive interneurons (stellate and basket cells)

Although stellate and basket cells in the molecular layer are known to be parvalbumin-positive (referred to as parvalbumin-positive interneurons throughout the text), in this study we used the NeuN staining to identify these cells. The advantage of the NeuN staining is that the immunopositive cell bodies are clearly visible against a dark background (the dendrites of the Purkinje cells and the parallel fibres, comprising most of the volume of the molecular layer, are NeuN negative). In the case of PV staining, by contrast, the immunopositive cells are often difficult to detect against the intense staining of the neuropil (Purkinje cell dendrites).

The density of stellate and basket cells in the molecular layer was significantly higher (+43%) in the mutant mice (Fig. 15).

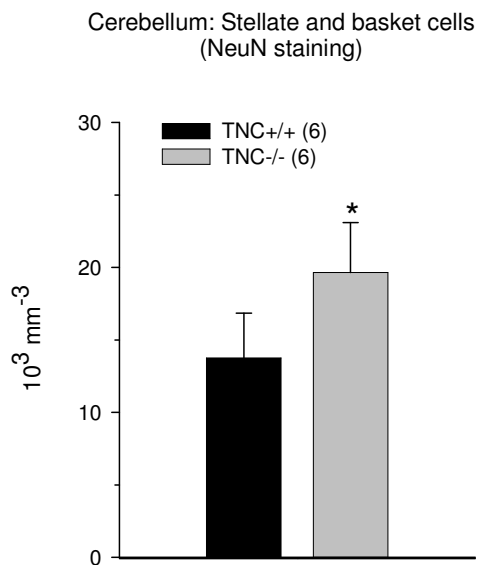


Figure 15: Density of stellate and basket cells in the cerebellum of TNC+/+ (black bars) and TNC-/- (grey bars) animals. Shown are mean values + SD. The number of animals studied per group is indicated in the legend. The asterisk indicates a significant difference between the two groups (*t*-test).

4.3.3.2 Purkinje neurons

The density of Purkinje neurons, identified by their size, position and positive staining for calbindin, was similar for both groups studied (Fig. 16).

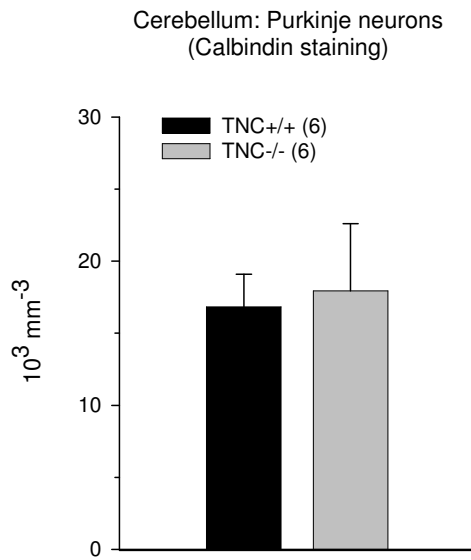


Figure 16: Density of Purkinje neurons in the cerebellum of TNC+/+ (black bars) and TNC-/- (grey bars) animals. Shown are mean values + SD. The number of animals studied per group is indicated in the legend. No significant difference was found (*t*-test).

4.3.4 Glial cells

4.3.4.1 Oligodendrocytes in the granular layer

The density of CNPase-positive cells in the granular layer was investigated and no difference between TNC-/- and TNC+/+ mice was found (Fig. 17).

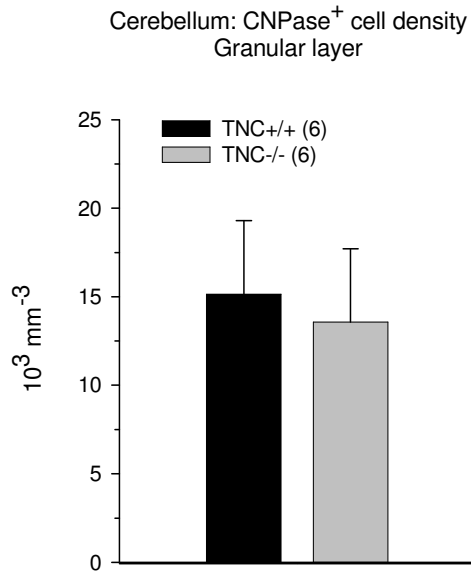


Figure 17: Density of oligodendrocytes in the granular layer of the cerebellum of TNC^{+/+} (black bars) and TNC^{-/-} (grey bars) animals. Shown are mean values + SD. The number of animals studied per group is indicated in the legend. No significant difference was found (*t*-test).

4.3.4.2 Astrocytes

The density of astrocytes was significantly increased (+40%) in both the molecular layer (Fig. 18) and the granular layer (Fig. 19) of the cerebellum of tenascin-C deficient mice. This finding is important, since the cerebellum is one more brain region, in addition to the neocortex, the hippocampus and the striatum (see above), with higher densities of astrocytes.

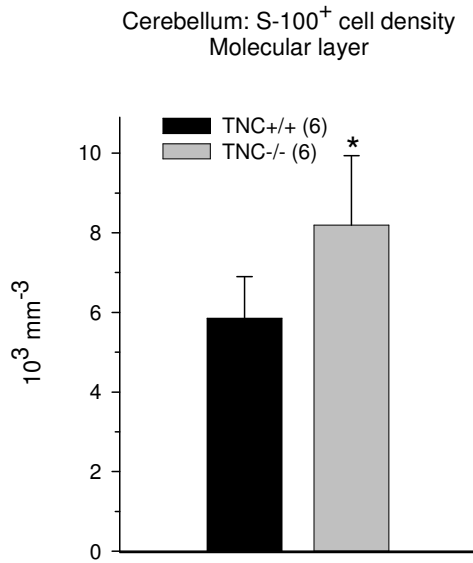


Figure 18: Density of astrocytes in the molecular layer of the cerebellum of TNC^{+/+} (black bars) and TNC^{-/-} (grey bars) animals. Shown are mean values + SD. The number of animals studied per group is indicated in the legend. The asterisk indicates a significant difference between the two groups (*t*-test).

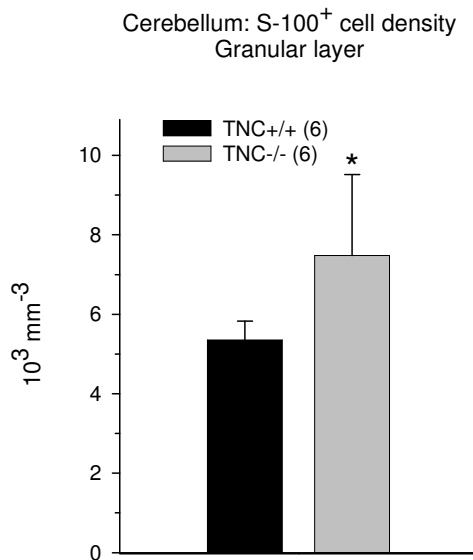


Figure 19: Density of astrocytes in the granular layer of the cerebellum of TNC^{+/+} (black bars) and TNC^{-/-} (grey bars) animals. Shown are mean values + SD. The number of animals studied per group is indicated in the legend. The asterisk indicates a significant difference between the two groups (*t*-test).

4.3.4.3 Microglia

The density of microglial cells in the molecular and the granular layer was studied separately, no difference between TNC deficient mice and wild-type mice being found (Fig. 20, Fig. 21).

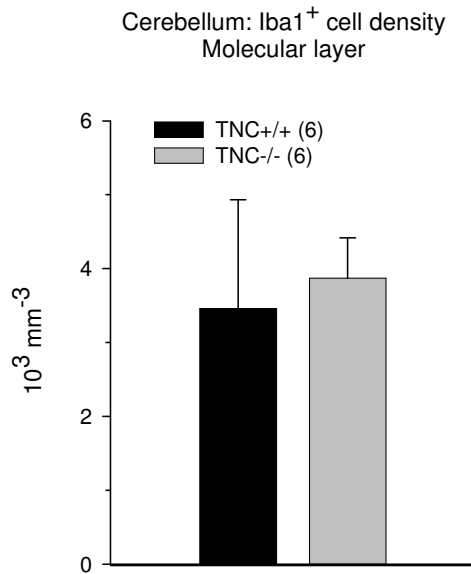


Figure 20: Density of microglial cells in the molecular layer of the cerebellum of TNC+/+ (black bars) and TNC-/- (grey bars) animals. Shown are mean values + SD. The number of animals studied per group is indicated in the legend. No significant difference was found (*t*-test).

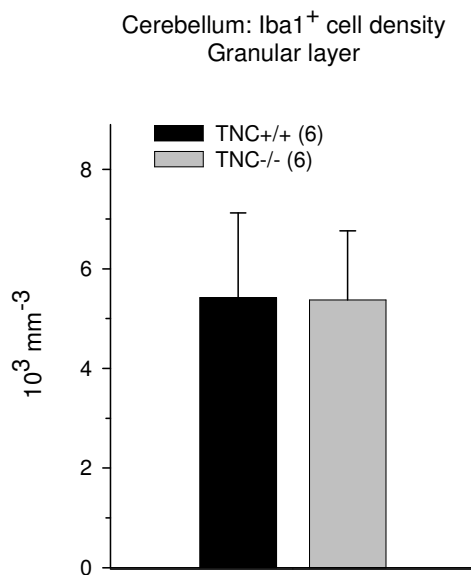


Figure 21: Density of microglial cells in the granular layer of the cerebellum of TNC+/+ (black bars) and TNC-/- (grey bars) animals. Shown are mean values + SD. The number of animals studied per group is indicated in the legend. No significant difference was found (*t*-test).

4.4 Purkinje cell size and synaptic inputs to Purkinje cells

Since stellate and basket cells are a major source of inhibitory synaptic inputs to Purkinje cell neurons, their abnormally high number raised the question as to whether synaptic inputs to Purkinje cells are different in TNC deficient mice. To answer this question, perisomatic and dendritic puncta positive for VGAT were quantified and the Purkinje cell size was measured.

4.4.1 Purkinje cell size

Digitised confocal images were used to estimate the size of the Purkinje cell bodies. Soma areas were similar in TNC^{-/-} and TNC^{+/+} mice (Fig. 22). From this observation it can be concluded that the linear density of perisomatic puncta (see below) is proportional to the numbers of puncta, i.e. synaptic input, per cell.

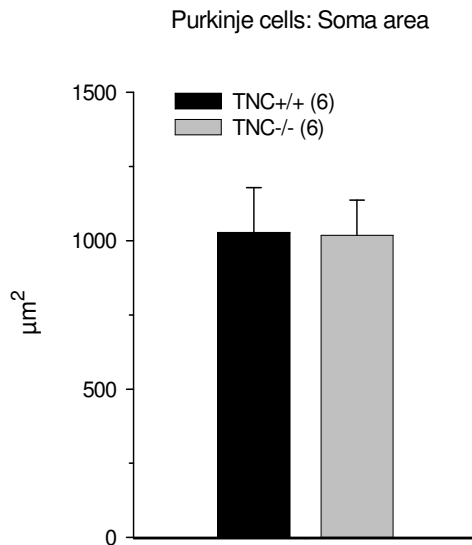


Figure 22: Purkinje cell size in the cerebellum of TNC^{+/+} (black bars) and TNC^{-/-} (grey bars) animals. Shown are mean values + SD. The number of animals studied per group is indicated in the legend. No significant difference was found (*t*-test).

4.4.2 Perisomatic puncta

Perisomatic inputs to Purkinje cells derive predominantly from basket cells (Spatkowski and Schilling 2003) and are inhibitory. The neuronal transmitter is GABA, which is why they can be detected by the VGAT staining. The results of the quantitative analysis showed no difference between TNC^{-/-} and TNC^{+/+} mice as regards the linear density (numbers per unit length) of VGAT⁺ terminals around Purkinje cells (Fig. 23).

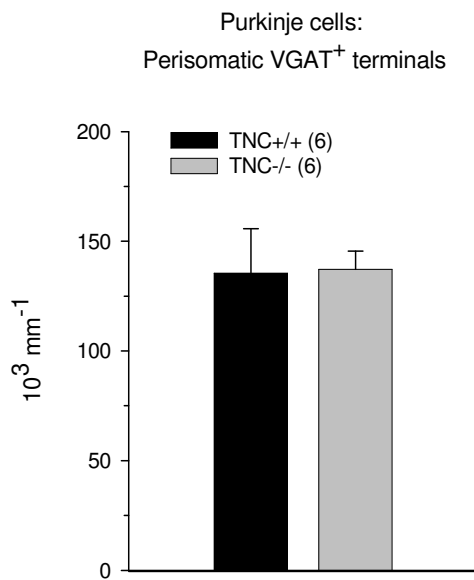


Figure 23: Linear density of perisomatic puncta (normalized to cell perimeter) around Purkinje cells in the cerebellum of TNC^{+/+} (black bars) and TNC^{-/-} (grey bars) animals. Shown are mean values + SD. The number of animals studied per group is indicated in the legend. No significant difference was detected (*t*-test).

4.4.3 Dendritic puncta

Estimates of VGAT⁺ profile densities in the molecular layer, these being predominantly stellate axon terminals (Spatkowski and Schilling 2003), showed no difference between TNC deficient and wild-type mice (Fig. 24).

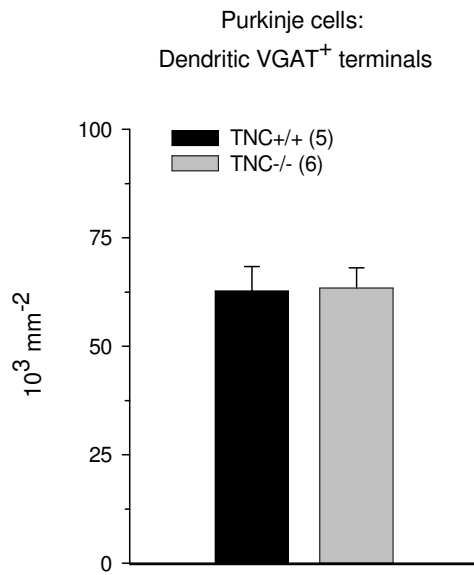


Figure 24: Density of dendritic puncta in the cerebellum of TNC^{+/+} (black bars) and TNC^{-/-} (grey bars) animals. Shown are mean values + SD. The number of animals studied per group is indicated in the legend. No significant difference was found (*t*-test).

5 DISCUSSION

The results of this study show that deficient expression of the ECM molecule tenascin-C in the mouse causes structural aberrations in the striatum and the cerebellum. Whereas gross morphological variables and synaptic coverage seemed to be unaltered, a number of genotype-specific differences in cell densities were detected. They provide novel evidence of the functional importance of the ECM molecule tenascin-C in the development of the striatum and the cerebellum. The major findings of this study are summarized in Table 1.

	Neostriatum	Cerebellum
Gross anatomical variables		
Volume or thickness of structures	= (volume)	= (thickness of layers)
Stereological analysis		
All cells	=	/
Major neuronal populations	= (medium spiny projection neurons)	= (Purkinje cells) = (granule cells)
PV ⁺ interneurons	↓	↑ (stellate and basket cells)
ChAT ⁺ interneurons	=	/
S-100 ⁺ astrocytes	↑	↑
CNPase ⁺ oligodendrocytes	=	=
Iba1 ⁺ microglial cells	=	=
Analysis of synaptic inputs		
Perisomatic VGAT ⁺ puncta	/	= (on Purkinje cells)
Dendritic VGAT ⁺ puncta	/	= (on Purkinje cells)

Table 1: Summary of genotype-related differences found in the striatum and the cerebellum. Arrows indicate significantly lower “↓” or higher “↑” values in TNC^{-/-} mice compared to TNC^{+/+} mice, “=” indicates that no significant difference was found, and “/” indicates that no analyses took place.

5.1 Gross morphological variables

Previous histological examination of tissue architecture by Saga et al. (1992) failed to detect abnormalities in tissue in which TNC is normally expressed, particularly thymus, lung and cerebellum. In the cerebellum, the thickness of the

granular and the Purkinje cell layer as well as the cell densities in these layers were found to be normal in TNC deficient mice. This is in agreement with our findings, which show normal granular layer thickness (Table 1), normal area of the striatum (Table 1) and normal thickness of the neocortex (Irintchev et al. 2005) in the mutant mouse. Altogether, these findings indicate that the gross morphology of the brain is not affected by constitutive ablation of TNC expression.

5.2 Stereological analysis of defined cell populations

The comprehensive stereological analysis of a variety of cell types provides a large and novel data set on the cellular composition of the striatum and the cerebellum in wild-type animals. These data are of interest, since such information, derived from simultaneous analysis of major cell types in the CNS, cannot be found in the literature. The only exception are two studies, one on the cerebral cortex of tenascin-C deficient and non-deficient mice (Irintchev et al. 2005) and a more recent study on the cerebellum of CHL1 deficient mice and wild-type littermates (Jakovcevski et al., manuscript in preparation) performed in our laboratory. Similar to this study, Jakovcevski et al. analyzed the densities of major neuronal and glial cell types in the cerebellum, but they investigated CHL1 deficient (CHL1^{-/-}) and wild-type (CHL1^{+/+}) mice. Their estimates of cell densities of granule cells, stellate and basket cells, Purkinje cells, astrocytes and microglia in wild-type mice are in good agreement with our results on wild-type animals.

In addition to producing data of general interest, we were able to identify a number of genotype-specific differences in cell densities (summarized in Table 1), which deserve special attention. The densities of parvalbumin-positive interneurons and astrocytes appeared to be altered in TNC^{-/-} mice, whereas the densities of all other neuronal and glial populations were found to be normal. This is in good agreement with a study on the cerebral cortex of TNC deficient mice, in which similarly, only a few cell populations, namely the total neuronal density and, as in this study, the density of PV⁺ interneurons and astrocytes, were found to be different, as compared to the mutant mice (Irintchev et al. 2005). Importantly, these differences in cell densities reflect differences in absolute cell numbers, since the area of the striatum and the

thickness of the molecular and the granular layer were similar in the two genotypes (see above). The aberrations in defined cell populations might well explain the observed abnormalities in physiology and behaviour of the TNC^{-/-} mice (see below).

5.2.1 Genotype-related aberrations of interneuron density in the striatum

The density of PV-positive interneurons in the striatum appeared to be specifically reduced in TNC^{-/-} as compared to wild-type animals (Table 1). In the cortex too, the density of PV⁺ interneurons has been found to be decreased and it has been ruled out that these differences simply reflect loss of immunoreactivity (Irintchev et al. 2005). With respect to these findings, the fact that most inhibitory cells are generated in and migrate tangentially into the striatum and the cortex from the medial ganglionic eminence (MGE) (Marín et al. 2000; Hamasaki et al. 2003; Métin et al. 2006) must be taken into account. Excitatory striatal projection neurons, by contrast, migrate radially from the lateral ganglionic eminence (LGE) (Hamasaki et al. 2003). Both inhibitory and excitatory striatal cell types are formed and start migrating at the end of the second and during the third embryonic week (Rodier 1980; Marín et al. 2000; Hamasaki et al. 2003), when TNC expression is barely detectable in the medial and the lateral ganglionic eminence (Gates et al. 1995). Interestingly, at this stage of development, regional differences in the specifications of neural stem cells, such as Pax6 expression, have been found between the MGE and the LGE. Pax6 regulates the combinatorial code of TNC isoform expression in the neural stem/progenitor cell complex (von Holst et al. 2007), which might result in differential regulatory functions of TNC in these brain regions. Since certain TNC isoforms, especially those of higher molecular mass, are thought to affect cell proliferation, in malignantly transformed cultured cells and carcinomas (Oyama et al. 1991; Ventimiglia et al. 1992; Tsunoda et al. 2003), for example, and probably also in cell cultures (Borsi et al. 1994), one can speculate that the generation of inhibitory interneurons in this region can be disturbed, given that these high-molecular isoforms are expressed to a higher extent in the MGE. Alternatively or in addition, since TNC affects apoptosis (Cowan et al. 2000; Garcion et al. 2001), ablation of the TNC gene might lead to abnormalities in cell numbers by

influencing the level of the naturally occurring cell death in specific regions, such as the MGE.

Given that TNC promotes cell migration, we can assume that tangential migration may be disturbed in the mutant mice. This assumption might explain both the decrease of PV⁺ interneurons in the striatum and the documented decrease of this cell population in the neocortex, because both PV-positive subpopulations are generated in the MGE and migrate tangentially, initially following a similar route (Marín et al. 2000).

One must also take into account, however, that cholinergic interneurons, which also migrate tangentially from the MGE (Hamasaki et al. 2003; Marín et al. 2000), were found to be normal in the mutant mice (Table 1). This suggests that TNC deficiency affects the specification and maturation of PV-positive interneurons at a later stage of development, after differentiation of precursor cells from the MGE into the various types of interneurons has already been completed. PV expression in a subpopulation of inhibitory neurons in the striatum and the cortex begins during the same developmental period, namely in the second postnatal week (Del Río et al. 1994, Alcantara et al. 1996; Schlosser et al. 1999). The chemical specification of the PV subpopulation of GABAergic neurons appears to be promoted by dopamine (Porter et al. 1999). Previous work has shown that the dopamine turnover rate is decreased in the striatum and the hippocampus (Fukamauchi et al. 1996) and that tyrosine hydroxylase activity is reduced in the striatum, the hippocampus and the cerebral cortex of TNC^{-/-} mice, suggesting lower dopamine levels (Fukamauchi et al. 1997). The lower number of PV⁺ cells may therefore be a consequence of a maturational deficit during postnatal development. And, interestingly, the dopamine turnover rate and tyrosine hydroxylase activity are normal in the cerebellum of TNC deficient mice (Fukamauchi et al. 1996; Fukamauchi et al. 1997), where the count of parvalbumin-positive interneurons showed no decrease, but rather an increase. In another study it has been directly shown that the number of parvalbumin-positive interneurons is reduced by dopaminergic ablation (Pezzi et al. 2005, but see also Trevitt et al. 2005). However, the cholinergic interneurons are not affected by the lack of dopamine innervation (Pezzi et al. 2005). We can therefore assume that low levels of dopamine do not disturb the specification

of cholinergic interneurons, so that this cell type should not be altered in the mutant mice; and indeed, these animals show a normal density of ChAT-positive cells.

Finally, we have to address the question as to the functional significance of the reduction of PV-positive interneurons in the striatum of TNC^{-/-} mice. Behavioural analyses have revealed motor deficits like hyperlocomotion and poor swimming ability in adult TNC deficient mice (Fukamauchi et al. 1996). Since GABAergic interneurons which co-express the calcium-binding protein parvalbumin provide the main source of inhibition and are involved in the synchronization of GABAergic spiny projection neurons (Koós and Tepper 1999; Ramanathan et al. 2002; Plenz 2003), they play an important role in the induction and suppression of movements. Loss of PV⁺ cells in the striatum due to perinatal asphyxia results in minor motor effects (Van de Berg et al. 2003). The subtle motor deficits reported for TNC^{-/-} mice, although in some aspects different from the deficits noticed in rats after asphyxia, might therefore also be attributable to a reduced density of PV-positive interneurons. It has already been shown that other motor disturbances, such as dystonias, a group of serious movement disorders characterized by involuntary contractions of opposing muscles, are based on a deficit of striatal PV⁺ interneurons leading to increased activity of striatal projection neurons (Gernert et al. 2000; Hamann et al. 2007). Furthermore, postmortem analysis of basal ganglia taken from individuals with Tourette syndrome, a childhood neuropsychiatric disorder characterized by persistent motor and vocal tics, i.e. sudden stereotyped motor sequences of varying intensity and complexity, has revealed lower densities of parvalbumin-positive interneurons in both the caudate nucleus and the putamen (Kalanithi et al. 2005).

5.2.2 Genotype-related aberrations of interneuron density in the cerebellum

In the cerebellum of tenascin-C deficient mice most cell populations were found to be normal, but a considerable increase in the density of PV-positive stellate and basket cells was detected (Table 1). These cells are formed by precursor cells in the white matter and migrate to the outer molecular layer during the first two postnatal weeks (Sotelo 2004; Yamanaka et al. 2004). In the white matter TNC is detectable

from birth until the third postnatal week, while in the molecular layer the expression of the glycoprotein starts at the time of birth and can still be observed in adult mice (Bartsch et al. 1992). In other words, initiation of TNC expression in the cerebellum coincides spatially and temporally with the formation and migration of the parvalbumin-positive interneurons in the cerebellum and could arguably influence their proliferation or the naturally occurring cell death in the postnatal period.

In contrast to the cerebellum, the number of PV⁺ cells in the striatum of TNC^{-/-} mice was decreased (see above). These region-specific effects of tenascin-C ablation may be attributed to the different origins of striatal and cerebellar inhibitory interneurons. The parvalbumin-immunoreactive interneurons of the striatum derive from the ganglionic eminences, the progenitors are thought to be two mitotically active cell populations in the ventricular zone (VZ) and the subventricular zone (SVZ) (Smart 1976; Fentress 1981). The PV-positive stellate and basket cells, by contrast, are formed in the white matter of the cerebellum. The intensity of TNC expression is higher in the white matter of the cerebellum than in the ganglionic eminences (Bartsch et al. 1992; Gates et al. 1995), which might indicate that region-specific effects on cell populations are due to different levels of expression. Taking into account that the striatum develops from the prosencephalon whereas the cerebellum arises from the rhombencephalon, we can assume non-uniform distribution of cellular receptors or ECM components interacting with TNC, resulting in different effects on cell proliferation, migration and differentiation. This argument may also hold for the different temporal expression of the glycoprotein. Low TNC expression in the lateral SVZ/striatal area can already be detected by embryonic day 17 (Gates et al. 1995), whereas in the cerebellum it can only be observed postnatally (Bartsch et al. 1992). It seems likely that the components of the ECM, and thus their interactions with TNC, change during the time window between late foetal and early postnatal development.

5.2.3 Genotype-related aberrations of glial cells in the striatum and the cerebellum

In the cerebellum, but also in the striatum (Table 1), the cortex (Irintchev et al. 2005) and the hippocampus (F. Kuang, A. Irintchev, personal communication), the

number of astrocytes was significantly higher in TNC deficient mice than in wild-type littermates. Astrogliosis, i.e. hyperplasia and/or hypertrophy of astroglial cells, is commonly associated with CNS injury due to trauma, degenerative diseases, excitotoxicity or intoxication (Eng and Ghirnikar 1994; Little and O'Callagha 2001; Garzillo and Mello 2002; Borges et al. 2003). Neurodegenerative causes involving an activated immune system can be ruled out in the case of TNC deficiency since densities of Iba1⁺ microglial cells were normal (Table 1).

Unlike oligodendrocyte precursors, which originate in restricted brain regions, astrocytes arise from many, if not all, domains of the neuroepithelium (Jacobsen and Miller 2003). In rodents, the first astrocytes are generated at the time of birth in the subventricular zone (Kakita 2001; Slezak and Pfrieder 2003) and thus migrate postnatally into overlying white and grey matter (Levison et al. 1993; Kakita 2001). As glial cells remain mitotically competent after differentiation, their proliferation could well be affected postnatally by TNC deficiency or factors such as altered cell numbers or synaptogenesis due to the absence of tenascin-C. If we take into account that astrocytes can actively eliminate synapses (Slezak and Pfrieder 2003), we can hypothesise that the increase in the number of astrocytes in the cerebellum of TNC^{-/-} mice might be a response to a presumptive increase in the number of synapses on Purkinje cells, due to an increased number of stellate and basket cells, i.e. a compensatory measure aimed at reducing the number of synapses to a normal level. Still, this cannot explain the alterations of astrocytes in the other brain regions of the mutant mice.

It has been shown that TNC can significantly reduce the proliferation rate of astrocytes in vitro (Holly et al. 2005). There is also evidence indicating that the glycoprotein has an influence on astrocyte proliferation and morphology in a paracrine/autocrine fashion (Nishio et al. 2003). As a result, it might be expected that tenascin-C deficiency should lead to enhanced astrocyte proliferation. Qualitative analysis of astroglial reaction to brain injury has suggested an altered response in TNC deficient mice, as compared to wild-type control animals (Steindler et al. 1995). One can therefore assume that the abnormal size of the astrocyte population in TNC^{-/-} animals is related to altered responsiveness to normal exogenous stimuli, due to dysfunctional self-regulatory mechanisms.

In contrast to astrocytes, the oligodendrocyte density in the striatum and cerebellum of mice deficient in TNC was found to be normal. As for the striatum, previous studies have shown that TNC deficiency in development leads to reduced oligodendrocyte precursor proliferation, but also to reduced cell death (Garcion et al. 2001). Our results support the view that the mechanisms controlling oligodendrocyte cell numbers are sufficiently balanced in the striatum so that this population is normally sized in the adult mouse (Table 1).

5.3 Synaptic coverage of Purkinje cells

Stellate and basket cells are two main sources of inhibitory input to Purkinje cells. They form synapses on distinct domains of the Purkinje cells; basket cells synapse on Purkinje cell bodies and Purkinje cell axon initial segments, and stellate cells form synapses on the smooth surface of Purkinje cell stem dendrites (Spatkowski and Schilling 2003). The number of these inhibitory GABAergic synaptic contacts was estimated from sections of the cerebellum stained for VGAT. Both the number of perisomatic puncta and number of puncta on Purkinje cell dendrites were similar for TNC^{-/-} mice and TNC^{+/+} mice (Table 1). The finding of structurally normal synaptic input to Purkinje cells is in good agreement with the subtle motor deficits detected in TNC knockout mice (Fukamauchi et al. 1996; Kiernan et al. 1999), which could be a consequence of the decrease in PV⁺ cell density in the striatum (see above). Considering that the number of stellate and basket cells was significantly higher in the mutant mice but that the number of synaptic contacts was normal, we can conclude that the mechanisms controlling the inhibitory input to Purkinje cells are balanced.

We also have to consider that astrocytes are known to regulate synapses on Purkinje cells (Seil 2001). Assuming that they can actively eliminate synapses (Slezak and Pfrieger 2003), we can hypothesise that reduction of synapses on Purkinje cells to a normal number is a consequence of a compensatory increase in astrocytes in the cerebellum of TNC^{-/-} mice (see above).

5.4 Concluding remarks

The results of this study show that TNC deficiency in mice leads to abnormalities in the size of interneuron populations and astrocytes in the neostriatum and cerebellum of adult mice. These findings clearly indicate that TNC is indispensable for normal brain development and provide a basis for further investigations aimed at elucidating the mechanisms underlying the formation and maintenance of specific cell populations in the CNS, and at determining how abnormalities in cell populations affect behaviour.

6 SUMMARY

Tenascin-C (TNC) is an extracellular matrix (ECM) glycoprotein abundantly expressed in neural and non-neural tissues during normal development, repair processes in the adult organism and tumourigenesis. In the central nervous system (CNS), it is produced by astrocytes and neuronal subpopulations and has been implicated in cell proliferation, neural cell migration, axonal growth and guidance, synaptic plasticity and neurotransmitter systems related to behaviour.

Mice deficient in TNC show a range of physiological and behavioural abnormalities. Previous studies have detected subtle structural abnormalities in the knockout mouse, most importantly alterations in neocortical cell populations. Especially with regard to the behavioural abnormalities documented, the question as to whether there are also morphological aberrations in the striatum and the cerebellum, both of which are involved in motor control, was raised. Alterations due to ablation of the TNC gene might give further insight into the functional role of the glycoprotein in CNS development and maturation.

We performed stereological estimations of immunohistochemically identified major cell types (neurons, neuronal subpopulations, astrocytes, oligodendrocytes and microglia) and morphometric analysis of the striatal volume and the thickness of the cerebellar cortex. Furthermore, the inhibitory GABA-mediated inputs to Purkinje cells were quantitatively analysed. Both TNC deficient (TNC^{-/-}) and non-deficient (TNC^{+/+}) mice were studied at the age of 5 months.

The results showed normal striatal volume and molecular and granular layer thickness in TNC deficient mice as well as normal total numbers of neurons and normal numbers of cholinergic interneurons, oligodendrocytes and microglia. In the striatum of TNC^{-/-} mice, a decrease in the number of parvalbumin-positive interneurons (-21%) was detected and astrocytes were more numerous than in wild-type littermates (+20%). In the cerebellum of adult TNC deficient mice, a marked increase in the number of PV⁺ interneurons (stellate and basket cells) was found (+43% compared to TNC^{+/+} littermates) and, as in the case of the striatum, the number of astrocytes was abnormally high in TNC^{-/-} mice (+40%). Perisomatic and dendritic

inhibitory inputs to Purkinje cells were similar in TNC deficient and wild-type animals.

The results of this study show that deficient expression of tenascin-C leads to the formation of an abnormally small population of PV⁺ interneurons in the striatum, what might be due to disturbances in tangential migration, cell proliferation and/or cell death during brain development and maturation. Loss of PV-positive interneurons may be partly responsible for previously reported behavioural deficits in TNC^{-/-} mice. In contrast to the striatum, the number of parvalbumin-positive stellate and basket cells in the cerebellum was markedly increased. This finding cannot be readily explained, but might be attributed to a different origin and a different level of tenascin-C expression along the migration route of stellate and basket cells, as compared to PV⁺ interneurons in the striatum. It seems likely that the abnormally high density of astrocytes in both brain regions is due to a loss of auto/paracrine control of astrocyte proliferation after TNC gene ablation.

This study shows that TNC deficiency in mice leads to abnormalities in the size of interneuron populations and astrocytes in the neostriatum and cerebellum of adult mice, which clearly indicates that the glycoprotein is indispensable for normal brain development.

7 REFERENCES

Alcantara S, de Lecea L, Del Rio JA, Ferrer I, Soriano E (1996) Transient colocalization of parvalbumin and calbindin D28k in the postnatal cerebral cortex: evidence for a phenotypic shift in developing nonpyramidal neurons. *Eur J Neurosci* 8:1329-1339

Andjus PR, Bajic A, Zhu L, Schachner M, Strata P (2005) Short-term facilitation and depression in the cerebellum: some observations on wild-type and mutant rodents deficient in the extracellular matrix molecule tenascin C. *Ann NY Acad Sci* 1048:185-197

Aufderheide E, Chiquet-Ehrismann R, Ekblom P (1987) Epithelial-mesenchymal interactions in the developing kidney lead to expression of tenascin in the mesenchyme. *J Cell Biol* 105:599-608

Aukhil I, Slemp CC, Lightner VA, Nishimura K, Briscoe G, Erickson HP (1990) Purification of hexabrachion (tenascin) from cell culture conditioned medium, and separation from a cell adhesion factor. *Matrix* 10:98-111

Barnea G, Grumet M, Milev P, Silvennoinen O, Levy JB, Sap J, Schlessinger J (1994) Receptor tyrosine phosphatase beta is expressed in the form of proteoglycan and binds to the extracellular matrix protein tenascin. *J Biol Chem* 269:14349-14352

Bartsch S, Bartsch U, Dörries U, Faissner A, Weller A, Ekblom P, Schachner M (1992) Expression of tenascin in the developing and adult cerebellar cortex. *J Neurosci* 12:736-749

Bartsch U (1996) The extracellular matrix molecule tenascin-C: expression in vivo and functional characterization in vitro. *Prog Neurobiol* 49:145-168

Bartsch U, Faissner A, Trotter J, Dörries U, Bartsch S, Mohajeri H, Schachner M (1994) Tenascin demarcates the boundary between the myelinated and nonmyelinated part of retinal ganglion cell axons in the developing and adult mouse. *J Neurosci* 14:4756-4768

Borges K, Gearing M, McDermott DL, Smith AB, Almonte AG, Wainer BH, Dingleline R (2003) Neuronal and glial pathological changes during epileptogenesis in the mouse pilocarpine model. *Exp Neurol* 182:21-34

Borsi L, Balza E, Castellani P, Carnemolla B, Ponassi M, Querze G, Zardi L (1994) Cell-cycle dependent alternative splicing of the tenascin primary transcript. *Cell Adhes Commun* 1:307-317

Bourdon MA, Ruoslahti E (1989) Tenascin mediates cell attachment through an RGD-dependent receptor. *J Cell Biol* 108:1149-1155

-
- Bourdon MA, Wikstrand CJ, Furthmayr H, Matthews TJ, Bigner DD (1983) Human glioma-mesenchymal extracellular matrix antigen defined by monoclonal antibody. *Cancer Res* 43:2796-2805
- Bristow J, Tee MK, Gitelman SE, Mellon SH, Miller WL (1993) Tenascin-X: a novel extracellular matrix protein encoded by the human XB gene overlapping P450c21B. *J Cell Biol* 122:265-278
- Brodkey JA, Laywell ED, O'Brien TF, Faissner A, Stefansson K, Dörries HU, Schachner M, Steindler DA (1995) Focal brain injury and upregulation of a developmentally regulated extracellular matrix protein. *J Neurosurg* 82:106-112
- Chaudhry FA, Reimer RJ, Bellocchio EE, Danbolt NC, Osen KK, Edwards RH, Storm-Mathisen J (1998) The vesicular GABA Transporter, VGAT, localizes to synaptic vesicles in sets of glycinergic as well as GABAergic neurons. *J Neurosci* 18:9733-9750
- Chiquet M, Fambrough DM (1984) Chick myotendinous antigen. II. A novel extracellular glycoprotein complex consisting of large disulfide-linked subunits. *J Cell Biol* 98:1937-1946
- Chiquet-Ehrismann R (1991) Anti-adhesive molecules of the extracellular matrix. *Curr Opin Cell Biol* 3:800-804
- Chiquet-Ehrismann R, Chiquet M (2003) Tenascins: regulation and putative functions during pathological stress. *J Pathol* 200:488-499
- Chiquet-Ehrismann R, Mackie EJ, Pearson CA, Sakakura T (1986) Tenascin: an extracellular matrix protein involved in tissue interactions during fetal development and oncogenesis. *Cell* 47:131-139
- Chiquet-Ehrismann R, Kalla P, Pearson CA, Beck K, Chiquet M (1988) Tenascin interferes with fibronectin action. *Cell* 53:383-390
- Chiquet-Ehrismann R, Hagios C, Schenk S (1995) The complexity in regulating the expression of tenascins. *Bioessays* 17:873-878
- Chung CY, Erickson HP (1994) Cell surface annexin II is a high affinity receptor for the alternatively spliced segment of tenascin-C. *J Cell Biol* 126:539-548
- Chung CY, Zardi L, Erickson HP (1995) Binding of tenascin-C to soluble fibronectin and matrix fibrils. *J Biol Chem* 270:29012-29017
- Chung CY, Murphy-Ullrich JE, Erickson HP (1996) Mitogenesis, cell migration, and loss of focal adhesions induced by tenascin-C interacting with its cell surface receptor, annexin II. *Mol Biol Cell* 7:883-892

Chuong CM, Crossin KL, Edelman GM (1987) Sequential expression and differential function of multiple adhesion molecules during the formation of cerebellar cortical layers. *J Cell Biol* 104:331-342

Cifuentes-Diaz C, Velasco E, Meunier FA, Goudou D, Belkadi L, Faille L, Murawsky M, Angaut-Petit D, Molgo J, Schachner M, Saga Y, Aizawa S, Rieger F (1998) The peripheral nerve and the neuromuscular junction are affected in the tenascin-C-deficient mouse. *Cell Mol Biol (Noisy-le-grand)* 44:357-379

Cleek RL, Rege AA, Denner LA, Eskin SG, Mikos AG (1997) Inhibition of smooth muscle cell growth in vitro by an antisense oligodeoxynucleotide released from poly(DL-lactic-co-glycolic acid) microparticles. *J Biomed Mater Res* 35:525-530

Conway JF, Parry DA (1991) Three-stranded alpha-fibrous proteins: the heptad repeat and its implications for structure. *Int J Biol Macromol* 13:14-16

Cowan KN, Jones PL, Rabinovitch M (2000) Elastase and matrix metalloproteinase inhibitors induce regression, and tenascin-C antisense prevents progression, of vascular disease. *J Clin Invest* 105:21-34

Crossin KL (1991) Cytotactin binding: inhibition of stimulated proliferation and intracellular alkalinization in fibroblasts. *Proc Natl Acad Sci USA* 88:11403-11407

Crossin KL, Hoffman S, Grumet M, Thiery JP, Edelman GM (1986) Site-restricted expression of cytotactin during development of the chicken embryo. *J Cell Biol* 102:1917-1930

Crossin KL, Hoffman S, Tan SS, Edelman GM (1989) Cytotactin and its proteoglycan ligand mark structural and functional boundaries in somatosensory cortex of the early postnatal mouse. *Dev Biol* 136:381-392

Crossin KL, Prieto AL, Hoffman S, Jones FS, Friedlander DR (1990) Expression of adhesion molecules and the establishment of boundaries during embryonic and neural development. *Exp Neurol* 109:6-18

De Chevigny A, Lemasson M, Saghatelian A, Sibbe M, Schachner M, Lledo PM (2006) Delayed onset of odor detection in neonatal mice lacking tenascin-C. *Mol Cell Neurosci* 32:174-186

Del Río JA, de Lecea L, Ferrer I, Soriano E (1994) The development of parvalbumin-immunoreactivity in the neocortex of the mouse. *Brain Res Dev Brain Res* 81:247-259

Eng LF, Ghirnikar RS (1994) GFAP and astrogliosis. *Brain Pathol* 4:229-237

Erickson HP, Bourdon MA (1989) Tenascin: an extracellular matrix protein prominent in specialized embryonic tissues and tumors. *Annu Rev Cell Biol* 5:71-92

-
- Erickson HP, Inglesias JL (1984) A six-armed oligomer isolated from cell surface fibronectin preparations. *Nature* 311:267-269
- Evers MR, Salmen B, Bukalo O, Rollenhagen A, Bösl MR, Morellini F, Bartsch U, Dityatev A, Schachner M (2002) Impairment of L-type Ca²⁺ channel-dependent forms of hippocampal synaptic plasticity in mice deficient in the extracellular matrix glycoprotein tenascin-C. *J Neurosci* 22:7177-7194
- Faissner A (1997) The tenascin gene family in axon growth and guidance. *Cell Tissue Res* 290:331-341
- Faissner A, Kruse J (1990) J1/tenascin is a repulsive substrate for central nervous system neurons. *Neuron* 5:627-637
- Faissner A, Steindler D (1995) Boundaries and inhibitory molecules in developing neural tissues. *Glia* 13:233-254
- Faissner A, Scholze A, and Götz B (1994) Tenascin glycoproteins in developing neural tissues: only decoration? *Perspect Dev Neurobiol* 2:53-66
- Fentress JC, Stanfield BB, Cowan WM (1981) Observation on the development of the striatum in mice and rats. *Anat Embryol (Berl)* 163:275-298
- Ferhat L, Chevassus au Louis N, Jorquera I, Niquet J, Khrestchatisky M, Ben-Ari Y, Represa A (1996) Transient increase of tenascin-C in immature hippocampus: astroglial and neuronal expression. *J Neurocytol* 25:53-66
- Forsberg E, Hirsch E, Frohlich L, Meyer M, Ekblom P, Aszodi A, Werner S, Fassler R (1996) Skin wounds and severed nerves heal normally in mice lacking tenascin-C. *Proc Natl Acad Sci USA* 93:6594-6599
- Franklin KBJ, Paxinos G (1997) *The mouse brain in stereotaxic coordinates*. Academic Press, California
- Fukamauchi F, Kusakabe M (1997) Preprotachykinin A and cholecystokinin mRNAs in tenascin-gene knockout mouse brain. *Neuropeptides* 31:199-201
- Fukamauchi F, Mataga N, Wang YJ, Sato S, Yoshiki A, Kusakabe M (1996) Abnormal behavior and neurotransmissions of tenascin gene knockout mouse. *Biochem Biophys Res Commun* 221:151-156
- Fukamauchi F, Mataga N, Wang YJ, Sato S, Yoshiki A, Kusakabe M (1997) Tyrosine hydroxylase activity and its mRNA level in dopaminergic neurons of tenascin gene knockout mouse. *Biochem Biophys Res Commun* 231:356-359
- Fukamauchi F, Aihara O, Kusakabe M (1998) Reduced mRNA expression of neuropeptide Y in the limbic system of tenascin gene disrupted mouse brain. *Neuropeptides* 32:265-268

Fuss B, Pott U, Fischer P, Schwab ME, Schachner M (1991) Identification of a cDNA clone specific for the oligodendrocyte-derived repulsive extracellular matrix molecule J1-160/180. *J Neurosci Res* 29:299-307

Fuss B, Wintergerst ES, Bartsch U, Schachner M (1993) Molecular characterization and in situ mRNA localization of the neural recognition molecule J1-160/180: a modular structure similar to tenascin. *J Cell Biol* 120:1237-1249

Garcion E, Faissner A and French-Constant C (2001) Knockout mice reveal a contribution of the extracellular matrix molecule tenascin-C to neural precursor proliferation and migration. *Development* 128:2485-2496

Garman RH (1990) Artifacts in routinely immersion fixed nervous tissue. *Toxicol Pathol* 18:149-153

Garzillo CL, Mello LE (2002) Characterization of reactive astrocytes in the chronic phase of the pilocarpine model of epilepsy. *Epilepsia* 43(Suppl 5):107-109

Gates MA, Thomas LB, Howard EM, Laywell ED, Sajin B, Faissner A, Götz B, Silver J, Steindler DA (1995) Cell and molecular analysis of the developing and adult mouse subventricular zone of the cerebral hemispheres. *J Comp Neurol* 361:249-266

Gernert M, Hamann M, Bennay M, Loscher W, Richter A (2000) Deficit of striatal parvalbumin-reactive GABAergic interneurons and decreased basal ganglia output in a genetic rodent model of idiopathic paroxysmal dystonia. *J Neurosci* 20:7052-7058

Götz B, Scholze A, Clement A, Joester A, Schütte K, Wigger F, Frank R, Spiess E, Ekblom P, Faissner A (1996) Tenascin-C contains distinct adhesive, anti-adhesive, and neurite outgrowth promoting sites for neurons. *J Cell Biol* 132:681-699

Götz M, Bolz J, Joester A, Faissner A (1997) Tenascin-C synthesis and influence on axonal growth during rat cortical development. *Eur J Neurosci* 9:496-506

Grumet M, Hoffman S, Crossin KL, Edelman GM (1985) Cytotactin, an extracellular matrix protein of neural and non-neural tissues that mediates glia-neuron interaction. *Proc Natl Acad Sci USA* 82:8075-8079

Guntinas-Lichius O, Angelov DN, Morellini F, Lenzen M, Skouras E, Schachner M, Irintchev A (2005) Opposite impacts of tenascin-C and tenascin-R deficiency in mice on the functional outcome of facial nerve repair. *Eur J Neurosci* 22:2171-2179

Hagios C, Koch M, Spring J, Chiquet M, Chiquet-Ehrismann R (1996) Tenascin-Y: a protein of novel domain structure is secreted by differentiated fibroblasts of muscle connective tissue. *J Cell Biol* 134:1499-1512

Hamann M, Richter A, Meillasson FV, Nitsch C, Ebert U (2007) Age-related changes in parvalbumin-positive interneurons in the striatum, but not in the sensorimotor cortex in dystonic brains of the dt(sz) mutant hamster. *Brain Res* 1150:190-199

-
- Hamasaki T, Goto S, Nishikawa S, Ushio Y (2003) Neuronal cell migration for the developmental formation of the mammalian striatum. *Brain Res Brain Res Rev* 41:1-12
- Holley JE, Gveric D, Whatmore JL, Gutowski NJ (2005) Tenascin C induces a quiescent phenotype in cultured adult human astrocytes. *Glia* 52:53-58
- Howard CV, Reed MG (1998) Unbiased stereology – three dimensional measurement in microscopy. Oxford: BIOS Scientific Publishers
- Husmann K, Faissner A, Schachner M (1992) Tenascin promotes cerebellar granule cell migration and neurite outgrowth by different domains in the fibronectin type III repeats. *J Cell Biol* 116:1475-1486
- Imai Y, Kohsaka S (2002) Intracellular signaling in M-CSF-induced microglia activation: role of Iba1. *Glia* 40:164-174
- Irintchev A, Salvini TF, Faissner A, Wernig A (1993) Differential expression of tenascin after denervation, damage or paralysis of mouse soleus muscle. *J Neurocytol* 22:955-965
- Irintchev A, Rollenhagen A, Troncoso E, Kiss JZ, Schachner M (2005) Structural and functional aberrations in the cerebral cortex of tenascin-C deficient mice. *Cereb Cortex* 15:950-962
- Jacobsen CT, Miller RH (2003) Control of astrocyte migration in the developing cerebral cortex. *Dev Neurosci* 25:207-216
- Jakovcevski I, Siering J, Hargus G, Hoelters L, Yin S, Schachner M, Irintchev A (to be published) Close homologue of L1 regulates numbers of Purkinje and granule cells during cerebellum development in mice. *J Comp Neurol*
- Jiao Y, Sun Z, Lee T, Fusco FR, Kimble TD, Meade CA, Cuthbertson S, Reiner A (1999) A simple and sensitive antigen retrieval method for free-floating and slide-mounted tissue sections. *J Neurosci Methods* 93:149-162
- Joester A, Faissner A (1999) Evidence for combinatorial variability of tenascin-C isoforms and developmental regulation in the mouse central nervous system. *J Biol Chem* 274:17144-17151
- Jones FS, Jones PL (2000) The tenascin family of ECM glycoproteins: structure, function, and regulation during embryonic development and tissue remodeling. *Dev Dyn* 218:235-259
- Jones FS, Burgoon MP, Hoffman S, Crossin KL, Cunningham BA, Edelman GM (1988) A cDNA clone for cytotactin contains sequences similar to epidermal growth factor-like repeats and segments of fibronectin and fibrinogen. *Proc Natl Acad Sci USA* 85:2186-2190

-
- Kakita A (2001) Migration pathways and behavior of glial progenitors in the postnatal forebrain. *Hum Cell* 14:59-75
- Kalanithi PS, Zheng W, Kataoka Y, DiFiglia M, Grantz H, Saper CB, Schwartz ML, Leckman JF, Vaccarino FM (2005) Altered parvalbumin-positive neuron distribution in basal ganglia of individuals with Tourette syndrome. *Proc Natl Acad Sci USA* 102:13307-13312
- Kiernan BW, Garcion E, Ferguson J, Frost EE, Torres EM, Dunnett SB, Saga Y, Aizawa S, Faissner A, Kaur R, Franklin RJ, French-Constant C (1999) Myelination and behaviour of tenascin-C null transgenic mice. *Eur J Neurosci* 11:3082-3092
- Koós T, Tepper JM (1999) Inhibitory control of neostriatal projection neurons by GABAergic interneurons. *Nat Neurosci* 2:467-472
- Kruse J, Keilhauer G, Faissner A, Timpl R, Schachner M (1985) The J1 glycoprotein - a novel nervous system cell adhesion molecule of the L2/HNK-1 family. *Nature* 316:146-148
- Langenfeld-Oster B, Faissner A, Irintchev A, Wernig A (1994) Polyclonal antibodies against NCAM and tenascin delay endplate reinnervation. *J Neurocytol* 23:591-604
- Laywell ED, Dörries U, Bartsch U, Faissner A, Schachner M, Steindler DA (1992) Enhanced expression of the developmentally regulated extracellular matrix molecule tenascin following adult brain injury. *Proc Natl Acad Sci USA* 89:2634-2638
- Leins A, Riva P, Lindstedt R, Davidoff MS, Mehraein P, Weis S (2003) Expression of tenascin-C in various human brain tumors and its relevance for survival in patients with astrocytoma. *Cancer* 98:2430-2439
- Levison SW, Chuang C, Abramson BJ, Goldman JE (1993) The migrational patterns and developmental fates of glial precursors in the rat subventricular zone are temporally regulated. *Development* 119:611-622
- Little AR, O'Callaghan JP (2001) Astroglialosis in the adult and developing CNS: is there a role for proinflammatory cytokines? *Neurotoxicology* 22:607-618
- Lochter A, Schachner M (1993) Tenascin and extracellular matrix glycoproteins: from promotion to polarization of neurite growth in vitro. *J Neurosci* 13:3986-4000
- Mackie EJ, Thesleff I, Chiquet-Ehrismann R (1987) Tenascin is associated with chondrogenic and osteogenic differentiation in vivo and promotes chondrogenesis in vitro. *J Cell Biol* 105:2569-2579
- Marín O, Anderson SA, Rubenstein JL (2000) Origin and molecular specification of striatal interneurons. *J Neurosci* 20:6063-6076

-
- Martini R (1994) Expression and functional roles of neural cell surface molecules and extracellular matrix components during development and regeneration of peripheral nerves. *J Neurocytol* 23:1-28
- Métin C, Baudoin JP, Rakic S, Parnavelas JG (2006) Cell and molecular mechanisms involved in the migration of cortical interneurons. *Eur J Neurosci* 23:894-900
- Milev P, Fischer D, Haring M, Schulthess T, Margolis RK, Chiquet-Ehrismann R, Margolis RU (1997) The fibrinogen-like globe of tenascin-C mediates its interactions with neurocan and phosphacan/protein-tyrosine phosphatase-zeta/beta. *J Biol Chem* 272:15501-15509
- Miragall F, Kadmon G, Faissner A, Antonicek H, Schachner M (1990) Retention of J1/tenascin and the polysialylated form of the neural cell adhesion molecule (N-CAM) in the adult olfactory bulb. *J Neurocytol* 19:899-914
- Morellini F, Schachner M (2006) Enhanced novelty-induced activity, reduced anxiety, delayed resynchronization to daylight reversal and weaker muscle strength in tenascin-C-deficient mice. *Eur J Neurosci* 23:1255-1268
- Moscoso LM, Cremer H, Sanes JR (1998) Organization and reorganization of neuromuscular junctions in mice lacking neural cell adhesion molecule, tenascin-C, or fibroblast growth factor-5. *J Neurosci* 18:1465-1477
- Nakao N, Hiraiwa N, Yoshiki A, Ike F, Kusakabe M (1998). Tenascin-C promotes healing of Habu-snake venom-induced glomerulonephritis: studies in knockout congenic mice and in culture. *Am J Pathol* 152:1237-1245
- Neidhardt J, Fehr S, Kutsche M, Lohler J, Schachner M (2003) Tenascin-N: characterization of a novel member of the tenascin family that mediates neurite repulsion from hippocampal explants. *Mol Cell Neurosci* 23:193-209
- Nies DE, Hemesath TJ, Kim JH, Gulcher JR, Stefansson K (1991) The complete cDNA sequence of human hexabrachion (Tenascin). A multidomain protein containing unique epidermal growth factor repeats. *J Biol Chem* 266:2818-2823
- Nishio T, Kawaguchi S, Iseda T, Kawasaki T, Hase T (2003) Secretion of tenascin-C by cultured astrocytes: regulation of cell proliferation and process elongation. *Brain Res* 990:129-140
- O'Brien TF, Faissner A, Schachner M, Steindler DA (1992) Afferent-boundary interactions in the developing neostriatal mosaic. *Brain Res Dev Brain Res* 65:259-267
- Oyama F, Hirohashi S, Shimosato Y, Titani K, Sekiguchi K (1991) Qualitative and quantitative changes of human tenascin expression in transformed lung fibroblast and lung tumor tissues: comparison with fibronectin. *Cancer Res* 51:4876-4881

-
- Pesheva P, Spiess E, Schachner M (1989) J1-160 and J1-180 are oligodendrocyte-secreted nonpermissive substrates for cell adhesion. *J Cell Biol* 109:1765-1778
- Pezzi S, Checa N, Alberch J (2005) The vulnerability of striatal projection neurons and interneurons to excitotoxicity is differentially regulated by dopamine during development. *Int J Dev Neurosci* 23:343-349
- Plenz D (2003) When inhibition goes incognito: feedback interaction between spiny projection neurons in striatal function. *Trends Neurosci* 26:436-443
- Porter LL, Rizzo E, Hornung JP (1999) Dopamine affects parvalbumin expression during cortical development in vitro. *J Neurosci* 19:8990-9003
- Prieto AL, Jones FS, Cunningham BA, Crossin KL, Edelman GM (1990) Localization during development of alternatively spliced forms of cytotoxin mRNA by in situ hybridization. *J Cell Biol* 111:685-698
- Prieto AL, Andersson-Fisone C, Crossin KL (1992) Characterization of multiple adhesive and counteradhesive domains in the extracellular matrix protein cytotoxin. *J Cell Biol* 119:663-678
- Ramanathan S, Hanley JJ, Deniau JM, Bolam JP (2002) Synaptic convergence of motor and somatosensory cortical afferents onto GABAergic interneurons in the rat striatum. *J Neurosci* 22:8158-8169
- Rathjen FG, Wolff JM, Chiquet-Ehrismann R (1991) Restrictin: a chick neural extracellular matrix protein involved in cell attachment co-purifies with the cell recognition molecule F11. *Development* 113:151-164
- Rettig WJ, Triche TJ, Garin-Chesa P (1989) Stimulation of human neuronectin secretion by brain-derived growth factors. *Brain Res* 487:171-177
- Rickmann M, Wolff JR (1995) Modifications of S100-protein immunoreactivity in rat brain induced by tissue preparation. *Histochem Cell Biol* 103:135-145
- Rocchi M, Archidiacono N, Romeo G, Saginati M, Zardi L (1991) Assignment of the gene for human tenascin to the region q32-q34 of chromosome 9. *Hum Genet* 86:621-623
- Rodier PM (1980) Chronology of neuron development: animal studies and their clinical implications. *Dev Med Child Neurol* 22:525-545
- Saga Y, Yagi T, Ikawa Y, Sakakura T, Aizawa S (1992) Mice develop normally without tenascin. *Genes Dev* 6:1821-1831
- Schlosser B, Klaus G, Prime G, Ten Bruggencate G (1999) Postnatal development of calretinin- and parvalbumin-positive interneurons in the rat neostriatum: an immunohistochemical study. *J Comp Neurol* 405:185-198

-
- Seil FJ (2001) Interactions between cerebellar Purkinje cells and their associated astrocytes. *Histol Histopathol* 16:955-968
- Siri A, Carnemolla B, Saginati M, Leprini A, Casari G, Baralle F, Zardi L (1991) Human tenascin: primary structure, pre-mRNA splicing patterns and localization of the epitopes recognized by two monoclonal antibodies. *Nucleic Acids Res* 19:525-531
- Slezak M, Pfrieder FW (2003) New roles for astrocytes: regulation of CNS synaptogenesis. *Trends Neurosci* 26:531-535
- Smart IH (1976) A pilot study of cell production by the ganglionic eminences of the developing mouse brain. *J Anat* 121:71-84
- Sotelo C (2004) Cellular and genetic regulation of the development of the cerebellar system. *Prog Neurobiol* 72:295-339
- Spatkowski G, Schilling K (2003) Postnatal dendritic morphogenesis of cerebellar basket and stellate cells in vitro. *J Neurosci Res* 72:317-326
- Spring J, Beck K, Chiquet-Erismann R (1989) Two contrary functions of tenascin: dissection of the active sites by recombinant tenascin fragments. *Cell* 59:325-334
- Steindler DA (1993) Glial boundaries in the developing nervous system. *Annu Rev Neurosci* 16:445-470
- Steindler DA, Cooper NG, Faissner A, Schachner M (1989) Boundaries defined by adhesion molecules during development of the cerebral cortex: the J1/tenascin glycoprotein in the mouse somatosensory cortical barrel field. *Dev Biol* 131:243-260
- Steindler DA, Settles D, Erickson HP, Laywell ED, Yoshiki A, Faissner A, Kusakabe M (1995) Tenascin knockout mice: barrels, boundary molecules, and glial scars. *J Neurosci* 15: 1971-1983
- Taylor HC, Lightner VA, Beyer WF Jr, McCaslin D, Briscoe G, Erickson HP (1989) Biochemical and structural studies of tenascin/hexabrachion proteins. *J Cell Biochem* 41:71-90
- Taylor J, Pesheva P, and Schachner M (1993). Influence of janusin and tenascin on growth cone behavior in vitro. *J Neurosci Res* 35:347-362
- Thesleff I, Mackie E, Vainio S, Chiquet-Ehrismann R (1987) Changes in the distribution of tenascin during tooth development. *Development* 101:289-296
- Trepel M (1995) *Neuroanatomie – Struktur und Funktion*, 1. Aufl., Urban & Schwarzenberg, München Wien Baltimore

-
- Trevitt JT, Morrow J, Marshall JF (2005) Dopamine manipulation alters immediate-early gene response of striatal parvalbumin interneurons to cortical stimulation. *Brain Res* 1035:41-50
- Tsunoda T, Inada H, Kalembeiyi I, Imanaka-Yoshida K, Sakakibara M, Okada R, Katsuta K, Sakakura T, Majima Y, Yoshida T (2003) Involvement of large tenascin-C splice variants in breast cancer progression. *Am J Pathol* 162:1857-1867
- Tucker RP (2001) Abnormal neural crest cell migration after the in vivo knockdown of tenascin-C expression with morpholino antisense oligonucleotides. *Dev Dyn* 222:115-119
- Tucker RP, Brunso-Bechtold JK, Jenrath DA, Khan NA, Poss PM, Sweatt AJ, Xu Y (1994) Cellular origins of tenascin in the developing nervous system. *Perspect Dev Neurobiol* 2:89-99
- Van de Berg WD, Kwaijtaal M, de Louw AJ, Lissone NP, Schmitz C, Faull RL, Blokland A, Blanco CE, Steinbusch HW (2003) Impact of perinatal asphyxia on the GABAergic and locomotor system. *Neuroscience* 117:83-96
- Vaughan L, Huber S, Chiquet M, Winterhalter KH (1987) A major, six-armed glycoprotein from embryonic cartilage. *EMBO J* 6:349-353
- Ventimiglia JB, Wikstrand CJ, Ostrowski LE, Bourdon MA, Lightner VA, Bigner DD (1992) Tenascin expression in human glioma cell lines and normal tissues. *J Neuroimmunol* 36:41-55
- Von Holst A, Egbers U, Prochiantz A, Faissner A (2007) Neural stem/progenitor cells express 20 tenascin C isoforms that are differentially regulated by Pax6. *J Biol Chem* 282:9172-9181
- Weber P, Montag D, Schachner M, Bernhardt RR (1998) Zebrafish tenascin-W, a new member of the tenascin family. *J Neurobiol* 35:1-16
- Wehrle-Haller B, Chiquet M (1993) Dual function of tenascin: simultaneous promotion of neurite growth and inhibition of glial migration. *J Cell Sci* 106:597-610
- Wolf HK, Buslei R, Schmidt-Kastner R, Schmidt-Kastner PK, Pietsch T, Wiestler OD, Blümcke I (1996) NeuN: A useful neuronal marker for diagnostic histopathology. *J Histochem Cytochem* 44:1167-1171
- Yamanaka H, Yanagawa Y, Obata K (2004) Development of stellate and basket cells and their apoptosis in mouse cerebellar cortex. *Neurosci Res* 50:13-22
- Yuasa S (1996) Bergmann glial development in the mouse cerebellum as revealed by tenascin expression. *Anat Embryol (Berl)* 194:223-23

8 ABBREVIATIONS

%	per cent
μ	micro (10 ⁻⁶)
°C	degrees Celsius
α	alpha
A	area
CA1	region in the hippocampus
Ca ²⁺	calcium ion
CaCl ₂	calcium chloride
CAM	cell adhesion molecule
CB	calbindin
ChAT	choline acetyltransferase
CHL1	close homologue of L1
CNPase	2', 3'-cyclic nucleotide 3'-phosphodiesterase
CNS	central nervous system
Cy3	carbocyanine 3 (red fluorescent carbocyanine)
ECM	extracellular matrix
e.g.	exempli gratia (for instance/for example)
EGFL	epidermal growth factor-like
est.	estimated
FNIII	fibronectin type three
g	gram
GABA	γ-amino butyric acid
GMEM	glial/mesenchymal extracellular matrix protein
h	hour
Iba1	ionized calcium-binding adaptor molecule
i.e.	id est (that is)
IgG	immunoglobulin G
i.p.	intraperitoneal
kDa	kilo Dalton
l	litre

LGE	lateral ganglionic eminence
LTP	long-term potentiation
M	molar
m	milli (10^{-3}), metre(s)
MGE	medial ganglionic eminence
min	minute(s)
mRNA	messenger ribonucleic acid
n	nano (10^{-9})
NaOH	sodium hydroxide
NeuN	neuron specific nuclear antigen
Pax6	paired box gene 6
PBS	phosphate buffered saline
pH	p(otential) of H(ydrogen), the logarithm of the reciprocal of hydrogen-ion concentration in gram atoms per litre
PV	parvalbumin
RGB	red, green and blue
RNA	ribonucleic acid
RPTP z/b	receptor protein tyrosine phosphatase beta/zeta
RT	room temperature
s	second(s)
SD	standard deviation
SPSS	Statistical Product and Service Solutions
SVZ	subventricular zone
S-100	low molecular weight calcium-binding protein expressed in astrocytes
T	distance
TA	tenascin assembly
TH	tyrosine hydroxylase
TN	tenascin
TNC	tenascin-C
TNC+/+	tenascin-C non-deficient (wild-type)
TNC+/-	tenascin-C heterozygous

TNC ^{-/-}	tenascin-C deficient
TNR	tenascin-R
V	volume
VGAT	vesicular GABA transporter
v/v	volume per volume
VZ	ventricular zone
w/v	weight per volume
ZMNH	Zentrum für Molekulare Neurobiologie Hamburg [Centre for Molecular Neurobiology]

9 ACKNOWLEDGEMENT/DANKSAGUNG

Die Arbeit wurde am Institut für Biosynthese neuraler Strukturen am Zentrum für molekulare Neurobiologie Hamburg (ZMNH) angefertigt. Bei Frau Prof. Dr. Melitta Schachner als Doktormutter und Direktorin des Instituts möchte ich mich für die Überlassung des interessanten Themas, für die Bereitstellung des Arbeitsplatzes und für die stete Hilfs- und Diskussionsbereitschaft herzlich bedanken.

Mein ganz besonderer Dank gilt Herrn Dr. Andrey Irintchev. Als mein Betreuer erklärte er mir die Grundlagen der Immunhistochemie und der stereologischen Analyse und beantwortete stets alle meine Fragen. Sowohl während des experimentellen Abschnitts als auch während des Schreibens genoss ich hervorragende Betreuung.

Frau Emanuela Szpotowicz danke ich herzlich für die Unterstützung beim Schneiden und Färben des Mausegewebes.

Ich möchte mich auch bei den Kollegen aus dem Labor bedanken, die mir den Umgang mit dem Mikroskop erklärten und immer gerne meine Fragen beantworteten.

Sehr herzlich möchte ich Frau Wiebke Bronrowan und Judit Alexandra Schroeter für das kritische und produktive Korrekturlesen danken.

Nicht zuletzt bedanke ich mich bei meinem Freund Birger Tobias Magesching, meinen Freunden und Kommilitonen und bei meiner Familie für ihre interessierte, verständnisvolle und geduldige Unterstützung.

10 CURRICULUM VITAE

Family name	Förster
First names	Janina Alexandra
Date of birth	July 2 nd 1983
Place of birth	Hamburg, Germany
Nationality	German

Education

Since 2002	Regular student of medicine, University of Hamburg
1993 – 2002	Secondary school: Hansa-Gymnasium, Hamburg-Bergedorf
1989 – 1993	Primary school: Ernst-Henning-Schule, Hamburg-Bergedorf

Exams

Sept. 2004	Physikum (pre-clinical examination)
June 2002	Abitur (German School-Leaving Certificate)

Dissertation

Since Oct. 2005	Quantitative morphological analysis of the striatum and the cerebellum of tenascin-C deficient mice, Zentrum für Molekulare Neurobiologie Hamburg, Institut für Biosynthese Neuraler Strukturen, Prof. Dr. Schachner
-----------------	--

11 EIDESSTATTLICHE VERSICHERUNG

Ich versichere ausdrücklich, dass ich die Arbeit selbständig und ohne fremde Hilfe verfasst, andere als die mir angegebenen Quellen und Hilfsmittel nicht benutzt und die aus den benutzten Werken wörtlich oder inhaltlich entnommenen Stellen einzeln nach Ausgabe (Auflage und Jahr des Erscheinens), Band und Seite des benutzten Werkes kenntlich gemacht habe.

Ferner versichere ich, dass ich die Dissertation bisher nicht an einen Fachvertreter an einer anderen Hochschule zur Überprüfung vorgelegt oder mich anderweitig um Zulassung zur Promotion beworben habe.

Hamburg, den

(Janina Alexandra Förster)